



저작자표시-비영리-변경금지 2.0 대한민국

이용자는 아래의 조건을 따르는 경우에 한하여 자유롭게

- 이 저작물을 복제, 배포, 전송, 전시, 공연 및 방송할 수 있습니다.

다음과 같은 조건을 따라야 합니다:



저작자표시. 귀하는 원저작자를 표시하여야 합니다.



비영리. 귀하는 이 저작물을 영리 목적으로 이용할 수 없습니다.



변경금지. 귀하는 이 저작물을 개작, 변형 또는 가공할 수 없습니다.

- 귀하는, 이 저작물의 재이용이나 배포의 경우, 이 저작물에 적용된 이용허락조건을 명확하게 나타내어야 합니다.
- 저작권자로부터 별도의 허가를 받으면 이러한 조건들은 적용되지 않습니다.

저작권법에 따른 이용자의 권리는 위의 내용에 의하여 영향을 받지 않습니다.

이것은 [이용허락규약\(Legal Code\)](#)을 이해하기 쉽게 요약한 것입니다.

[Disclaimer](#)

Master's Thesis

**Programmable activation of mechanical  
metamaterial using stiffness controllable  
mechanical pixels**

Jeeyoon Yi

Department of Materials Science and Engineering

Graduate School of UNIST

2020

**Programmable activation of mechanical  
metamaterial using stiffness controllable  
mechanical pixels**

Jeeyoon Yi

Department of Materials Science and Engineering

Graduate School of UNIST

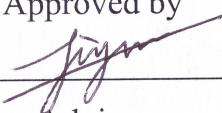
**Programmable activation of mechanical  
metamaterial using stiffness controllable  
mechanical pixels**

A thesis/dissertation  
submitted to the Graduate School of UNIST  
in partial fulfillment of the  
requirements for the degree of  
Master of Science

Jeeyoon Yi

12/12/2019

Approved by

  
\_\_\_\_\_  
Advisor

Jiyeon Kim

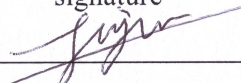
**Programmable activation of mechanical  
metamaterial using stiffness controllable  
mechanical pixels**

Jeeyoon Yi

This certifies that the thesis/dissertation of Jeeyoon Yi is approved.

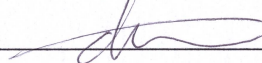
12/12/2019

signature



Advisor: Jiyun Kim

signature



Moon Kee Choi

signature



Young Chul Jun

## **Abstract**

Soft materials with negative Poisson's ratio, also known as auxetics, have been studied since they have unique and unusual mechanical properties induced by abrupt instability under applied external pressure. For instance, periodic void array in 2D structure is one of the common auxetic structures that have been studied with making a variation with changing void's shape or porosity<sup>24-26</sup>. However, formal research on auxetic materials focus on the structural changes. Therefore, coupling the material's characteristics and unique structures of auxetics would pave the way to develop advanced mechanical metamaterials.

Here, I developed a mechanical metamaterial with void array integrated with smart materials. Through this approach, I could actively control the macroscopic properties of the engineered material through modifying the stiffness of voids. Each void is comprised of three distinct layers, which are a conductive heating layer, phase-transition layer, and silicone rubber layer. Two electric wires are embedded in the conductive heating layer to make control of each void's stiffness, and these voids are named as mechanical pixel. The phase transition layer is the core element in this structure because it is stiff when they are in solid phase and become compliant when they are in liquid phase. This layer melts down when the conductive heating layer are heated through Joule heating. Availability of pixelated control of each conductive heating layer, this offer tunable material attribute to the conventional auxetic structure. The programmable activation of the structure provides me to exhibit diverse patterned deformation, and fixation of the deformed shape.

I believe these combined properties of materials, and the unusual structure (mechanical metamaterial) will give a novel design and idea to other soft material-based systems, such as wearable devices and soft robotics.



**Table of contents****CHAPTER 1 Introduction**

1.1 Mechanical Metamaterials-----	12
1.1.1. Extremal materials-----	13
1.1.2. Negative materials-----	15
1.1.3. Origami-based metamaterials-----	16
1.1.4. Active/programmable metamaterials-----	17
1.2 Mechanical metamaterials with patterned structure-----	18
1.3 Stiffness changing smart materials-----	21
1.4 Mechanical metamaterial with pixelated activation units-----	22
1.5 Outline of the research-----	24

**CHAPTER 2 Fabrication methods & materials-----25**

2.1 Mold design & printing-----	25
2.2 Fabrication of functional layers-----	26
2.2.1. Mold for silicone rubber layer-----	26
2.2.2. Pillars for the conductive heating layer-----	27
2.2.3. Pre-mold and mold for the LMPA layer-----	27
2.3 Assembly of layers-----	27
2.3.1. Fabrication of conductive heating layer-----	28
2.3.2. Fabrication of phase-transition layer-----	29
2.4 Layer characterizations-----	30
2.4.1. Attachment of the conductive heating layer on the pillar-----	30
2.4.2. Putting together the LMPA layer and the pillar-----	30
2.4.3. Silicone rubber layer-----	31
2.4.4. Arrangement of electric wires-----	32



2.5 Characterization of functional layers-----	32
2.5.1. The electrical conductivity of the conductive heating layer-----	32
2.5.2. The electrical resistance corresponding to the connected number of voids-----	34
2.5.3. Repetitive operation of the system and the temperature profiles-----	35
2.5.4. Heat transfer of the system-----	36
<b>CHAPTER 3 Structure activation &amp; actuation-----</b>	<b>37</b>
3.1 Operation cycle-----	37
3.1.1. Operation setting-----	37
3.1.2. Activation of a single unit-----	38
3.1.3. Operation cycle-----	39
3.2 Activation of metamaterials-----	41
3.3 Fixation of metamaterials-----	43
3.3.1. Reconfiguration cycle-----	43
3.3.2. Fixation of domain deformation of metamaterial-----	43
3.4 Conclusion-----	44
<b>CHAPTER 4 Poisson's ratio &amp; analysis-----</b>	<b>45</b>
4.1 Calculation-----	45
4.2 Comparison between silicone rubber structure-----	46
<b>CHAPTER 5 Concluding remarks-----</b>	<b>47</b>
5.1 Summary of the work-----	47
5.2 Future prospect-----	47
References-----	48
Acknowledgment-----	51
Curriculum Vitae-----	52

## List of figures

Figure 1 Additive manufacturing and mechanical metamaterials with diverse size scales-----	12
Figure 2 Penta-mode mechanical metamaterial-----	14
Figure 3 Dilational mechanical metamaterial-----	14
Figure 4 Negative linear compressibility material-----	15
Figure 5 The structure that embedding negative stiffness materials in a positive stiffness matrix-----	16
Figure 6 The structure of Miura-ori origami-----	16
Figure 7 Programmable mechanical metamaterials-----	18
Figure 8 Two limitations of formal programmable mechanical metamaterials-----	18
Figure 9 The negative Poisson's ratio and conventional honeycomb structures-----	19
Figure 10 Three patterned designs of re-entrant honeycomb structures-----	19
Figure 11 Samples of three patterned re-entrant honeycomb structures-----	20
Figure 12 LMPA embedded soft gripper and actuator-----	21
Figure 13 Honeycomb structure and graphene-based structure embedding LMPA-----	22
Figure 14 Periodic void structure with embedded LMPA layers-----	23
Figure 15 Pixelated programmable mechanical metamaterial-----	26
Figure 16 Film applicator and the mixture of carbon black and silicone rubber-----	28
Figure 17 Fabrication of LMPA layer-----	29
Figure 18 Assembly of pillars, conductive heating layers, and LMPA layer-----	30
Figure 19 Liquid silicone rubber poured into the mold-----	31
Figure 20 Arrangement of electric wires-----	32
Figure 21 Electrical conductivity according to the concentration of carbon black-----	33
Figure 22 The resistance of the structure according to the connected number of voids-----	34
Figure 23 The temperature change of single void depending on activation and applied voltage-----	35

Figure 24 Temperature change of the voids near the activated void-----	36
Figure 25 DC power supply-----	37
Figure 26 Local activation and deformation of a single mechanical pixel-----	38
Figure 27 The whole cycle of pixelated activation and deformation of the mechanical metamaterial--	40
Figure 28 Diverse patterned deformation of the pixelated mechanical metamaterial-----	42
Figure 29 Fixation of the compressed domain in the cycle of activation of the structure-----	43
Figure 30 Four fixed patterns of the structure-----	44
Figure 31 Comparison of Poisson's ratio of engineered structure and silicone rubber structure-----	45
Figure 32 Deformed engineered structure and silicone rubber structure-----	46

## List of abbreviations

<b>Abbreviation</b>	<b>Definition</b>
PDMS	Poly (dimethyl siloxane)
LMPA	Low Melting Point Alloy
B	Bulk modulus;
G	Shear modulus;

## CHAPTER 1 Introduction

This chapter explains the definition of mechanical metamaterials, the categories and examples of the mechanical metamaterials, existing researches on responsive mechanical metamaterials, locally activating mechanical metamaterials, and outline of the research.

### 1.1. Mechanical Metamaterials

The development of materials has been focused on changing the composition of materials rather than its structures during the past centuries. Even the human's history is divided by the most developed material of that era; thus, there are the ages called bronze age, iron age, and age of steel. Conventional materials are sharing similar properties compare to the novel materials, which are focusing on the design of the structures. One of those properties is positive Poisson's ratio, which materials with positive Poisson's ratio elongates its width when they are stretched and shrink its width when compressed. However, relatively recent years, the materials with unusual properties on familiar mechanical properties such as Poisson's ratio, Young's modulus, shear and bulk moduli have been developed. Those materials are artificially made, that cannot be observed in nature, and called 'metamaterials.' Their unique properties do not come from material composition, but their structural geometry. Several categories of metamaterials have been made and observed, such as optical, acoustic, and mechanical metamaterials. In specific, the definition of '*mechanical metamaterial*' is the materials that has artificial structures with mechanical properties defined by their structure rather than their composition.<sup>1-2</sup>

The recent advancement of technology further progressed the advance of diverse metamaterials, although the combining structural change into materials may not be new. For example, 3D printing technology such as additive manufacturing (AM) allows us to make more complicated structure materials with varied length scale (**Figure 1**).

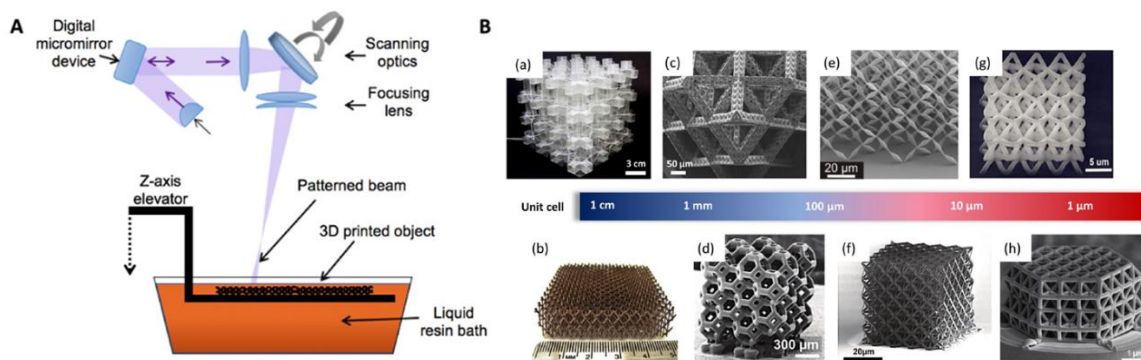


**Figure 1** The figure of additive manufacturing method and the diverse mechanical metamaterials structure with different size scales.

Size down the structure to nanoscale arouses the benefit to the materials that are called size-effect. When the same shape of the structure made in nanoscale, the mechanical strength becomes high compared to that of bulk structure.<sup>3</sup>

There are dozens of mechanical metamaterials categories, but this thesis will describe mechanical metamaterials with an unprecedented range of elastic mechanical properties with a large deformation range. Thus, we will focus on the mechanical metamaterials' categories of extremal materials, negative materials, origami (paper folding) metamaterials, and active/programmable metamaterials.<sup>4</sup>

### 1.1.1. Extremal materials

These materials were introduced in 1995 by Milton and Cherkaey. The definition of extremal materials is that those materials are extremely stiff in specific modes of deformation but extremely compliant in other modes. The eigenvalues of the elasticity tensor determine the behavior of the materials under any mode of deformation. The extremely compliant material has a very small eigenvalue when the material deformed in the direction according to the certain eigenvalue. The extremal materials categorized by the number of very small eigenvalues of the elasticity tensor, such as uni-mode(one very small eigenvalue), bi-mode, tri-mode, or quadra-mode. The combination of a very stiff phase and a very compliant phase is composing extremal materials, and this result makes us fabricate these materials through a 3D printer with stiff and compliant materials.<sup>5</sup>

Examples of extremal materials are Pentamode metamaterials and Dilational materials. Pentamode metamaterials are very stiff in one direction out of six direction, and compliant in the other five directions. From its property, the materials have large bulk modulus compare to shear modulus, so that it is hard to make a change in volume. Thus, the Poisson's ratio of Pentamode metamaterials is about 0.5. The behavior of the Pentamode metamaterial is similar to the fluid so that this material is also called as 'meta-fluids'<sup>6</sup> (**Figure 2**).

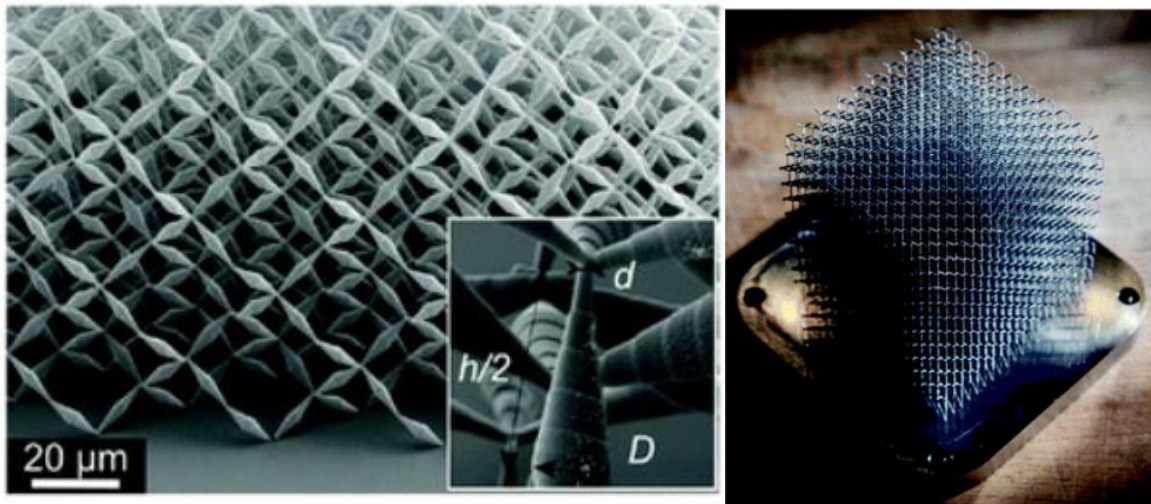


**Figure 2** The micro-scale structure of penta-mode mechanical metamaterial and it's whole structure.

Dilational materials have extremely high shear modulus compared to the bulk modulus, according to the following equation, when the  $B$  is the bulk modulus,  $G$  is the shear modulus, and  $\nu$  is the Poisson's ratio<sup>7</sup> (**Figure 3**).

From equation (1), both  $B$  and  $G$  are positive since elastic tensor must be positively defined. Therefore the value of Poisson's ratio is defined between  $-1$  to  $0.5$ . The Pentamode metamaterials are defined when the Poisson's ratio is  $0.5$ , which shows extremely high bulk modulus compared to the shear modulus. Unlike Pentamode metamaterials, the Dilational materials have Poisson's ratio of  $-1$  so that it has extremely low bulk modulus compared to the shear modulus. From these properties, the shape of the Dilational materials do not change irrespectively to how much deformation they undergo, but only changes their size. Thus, we can conclude the Pentamode metamaterials and Dilational materials are opposite in their characteristics.

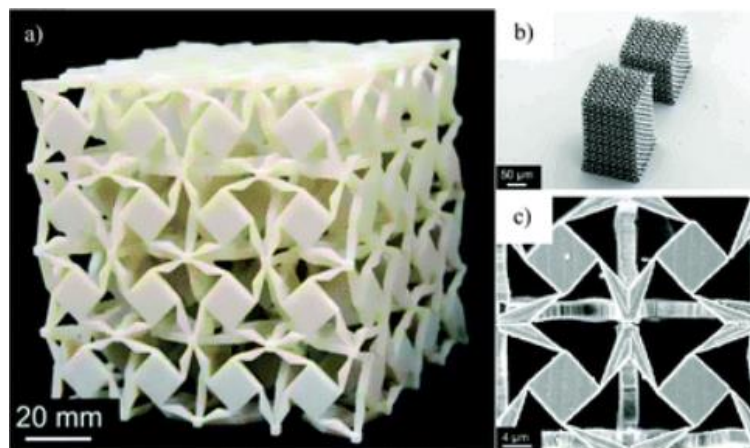


**Figure 3** Example figures of dilational mechanical metamaterials.

### 1.1.2. Negative materials

Negative metamaterials are materials that have negative moduli, such as the negative elastic modulus or the negative bulk modulus. Since the elasticity tensor (the bulk modulus and the shear modulus) should be positive as aforementioned, displaying negative moduli metamaterials shows unique mechanical behavior compare to extremal metamaterials.<sup>4</sup>

The metamaterial with the negative compressibility is the example of negative materials. Mostly compressibility is defined with three types of compressibilities: line, area, and volume compressibility. Depending on the type of compressibilities, the materials change in length, the area, and the volume of materials under applied hydrostatic pressure. Negative compressibility materials expand in their length, area, and volume under hydrostatic pressure. According to the number of dimensions of compressibility, the materials might undergo a change in their length, area, or volume<sup>4</sup> (**Figure 4**).

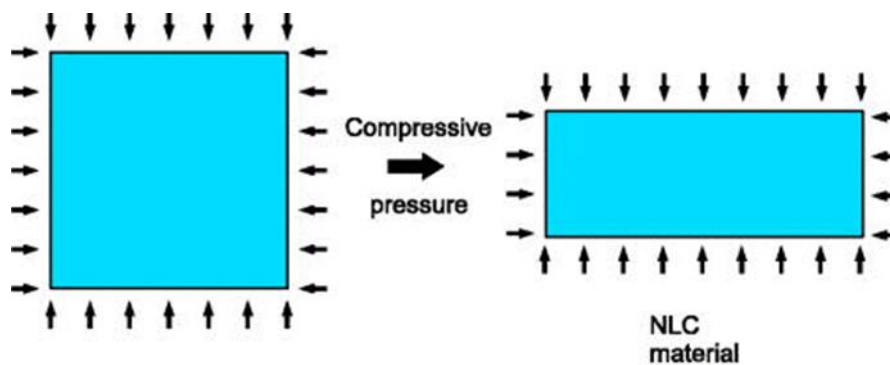


**Figure 4** The figure is showing negative linear compressibility material. This materials expand it's length when pressure is applied to the materials.

Materials with negative stiffness deform in the opposite direction of applied pressure and form an assisting force to assist the deformation, unlike materials with positive stiffness. Thus, negative stiffness materials undergo large deformations compared to the positive stiffness materials. Even negative stiffness materials can be combined or embedded within positive stiffness materials; we can utilize this combination of materials in diverse applications with their properties such as high damping coefficients<sup>8-11</sup> (**Figure 5**).

In the usual case, materials with high stiffness do not have high damping ratios as well as materials with high damping ratios are compliant. However, the negative stiffness materials are having a high damping ratio and high stiffness at the same time by embedding negative stiffness materials as inclusion in a positive stiffness matrix<sup>8-11</sup> (**Figure 5**). The positive stiffness materials ensure the stability of the combination while the inclusion of negative stiffness materials endowing very high damping coefficients. The materials with a high damping coefficient and high stiffness can be applied to vibration isolation.<sup>4</sup> The other application is using the metamaterials for transformation acoustic applications.



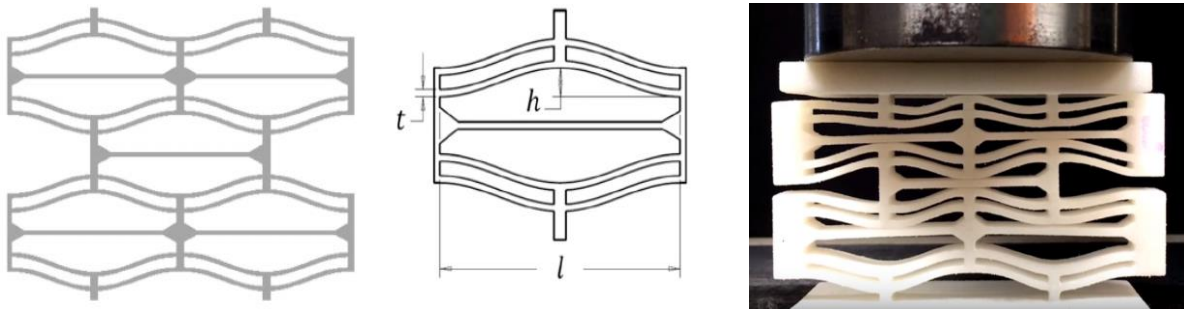


**Figure 5** The structure that embedding negative stiffness materials in a positive stiffness matrix.

### 1.1.3. Origami-based metamaterials

The metamaterials which are inspired by the ancient Japanese paper folding (Origami) are the new paradigms in the design and manufacturing of mechanical metamaterials. Origami-based metamaterials are having diverse applications in self-folding robots<sup>12</sup>, medical stents<sup>13</sup>, and mechanical metamaterials<sup>14</sup>. In the applications, the metamaterial is originally flat and made of various types of materials that could be activated to self-fold to a targeted (three-dimensional) shape. The deformed shapes are different in their geometries, mechanical properties, and functions, depending on the design and folding patterns of origami metamaterials. Origami structure can be subdivided into pure origami and rigid origami. Pure origami always starts from a square sheet and deformed without any cuts in the paper or any use of glue. In rigid origami, the folding lines are considered as kinematic joints so that the process of folding can be achieved with the reduced kinematic process with a lot of constraints. Another concept that is closely related to origami is called kirigami that allows for cuts, unlike origami.

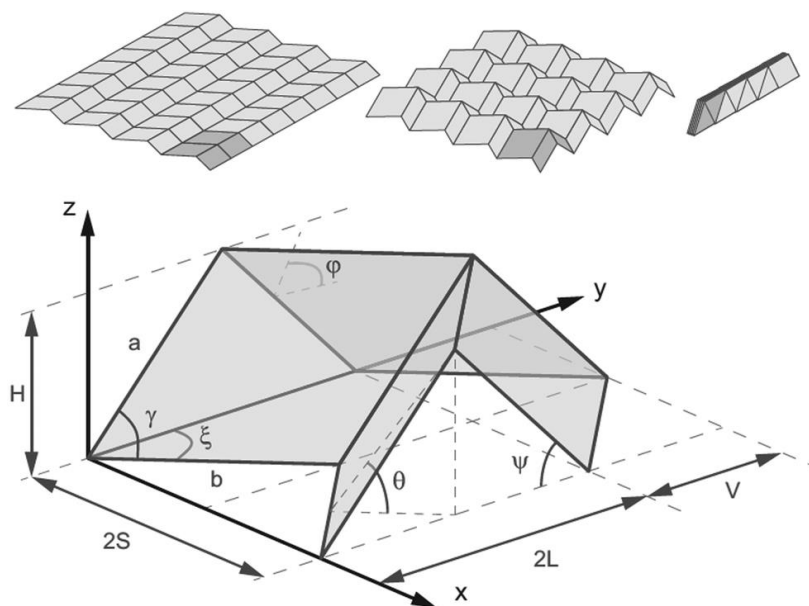


**Figure 6** The structure of Miura-ori origami, which is the most widely studied origami.

The most widely studied origami structures are Miura-ori origami<sup>15</sup> (**Figure 6**). Metamaterials fabricated based on the Miura-ori origami structure have been exhibited negative Poisson's ratio, and some variants in the structures have been used for developing reprogrammable mechanical metamaterials.<sup>16</sup> From the examples of origami-based metamaterials, this novel category of metamaterial is a promising area with many spaces and new features to develop in the mechanical metamaterial field.

#### 1.1.4. Active/programmable metamaterials

Active and programmable metamaterials are usually made of soft materials, having large deformations, and instability. A wide range of designs of mechanical metamaterials has been developed by combining these three concepts. For example, metamaterials could achieve unprecedented properties or functionalities through harness the instability of soft materials in the nonlinear deformation range. Active and programmable mechanical metamaterials are coming from the studies on the instability regimens of soft and patterned materials.<sup>4</sup>

The magnetic field responsive metamaterial shows the programmable stiffness depending on the existence of an applied magnetic field<sup>17</sup> (**Figure 7**). These mechanical metamaterials are printed with the 3D printer with hollow beam structures, and magnetic particles are injected into the structure. Then particles self-assembled to stiffening the entire structure upon the application of the external magnetic field. Although some programmable metamaterials are made of one material, it exhibits different phase under pressure. Metamaterials with ferro-elasticity were made of soft silicone rubber and fabricated in a vacuum chamber<sup>18</sup> (**Figure 7**). Under the atmospheric pressure, the periodic void array with two different sizes exhibits buckling with two different variants. Since these variants can co-exist, the researchers of the study called this ferro-elasticity, which can reversibly change its deformed state by applying pressure. 4D printing responsive metamaterials are also the example of programmable metamaterials.<sup>19</sup> For example, the mechanical metamaterials consist of temperature-responsive shape memory polymer are shape programmable structure. The materials are in the glassy state under low temperature, and in the rubbery state under high temperature. Thus, by twisting or recovering the shape of the mechanical metamaterials according to temperature changes, researchers can variably change the shape of the structure.

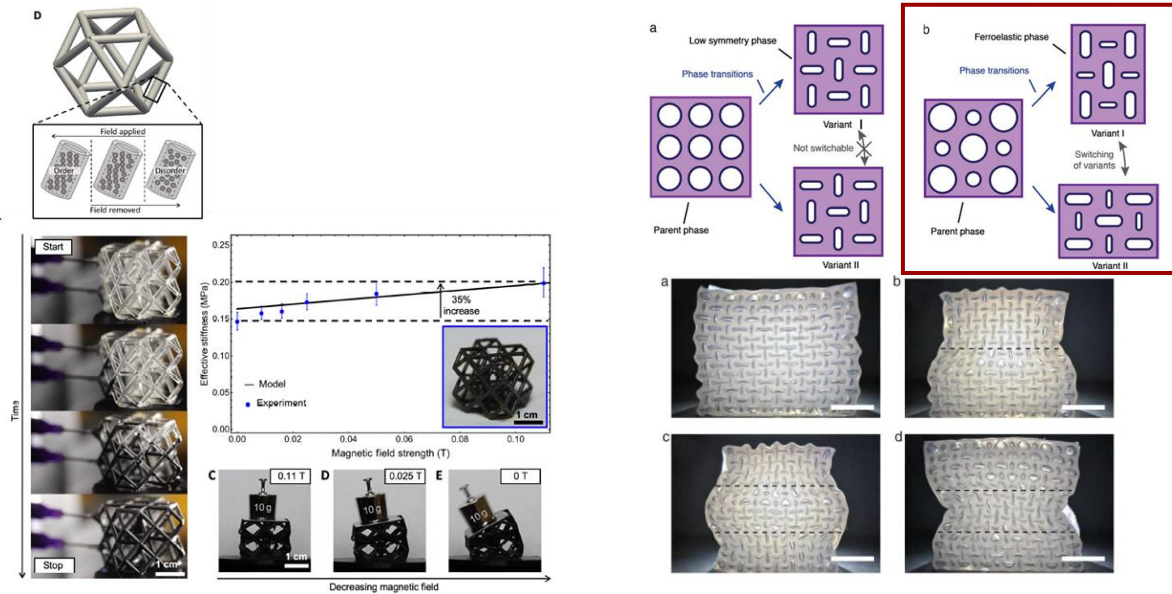


**Figure 7** The mechanical metamaterials showing programmability through changing stiffness depending on the applied magnetic field, and changing the variants under the atmospheric pressure.

## 1.2. Mechanical metamaterials with patterned structure

The limitations of formal studies of mechanical metamaterial are lack of local activation and pre-determined shape deformation. Formal programmable metamaterials are showing property changes under stimuli; however, these changes have happened in the entire structure. To make more complicated and higher programmability, the new programmable metamaterials should have local property changing characters (**Figure 8**). Also, formal researches are having pre-determined deformation, in which the structure is deformed in only one fixed shape under stimuli. For instance, the 4D printed flower-shaped structures can be curled or twisted its petals depending on the printed patterns when they get moisture<sup>20</sup> (**Figure 8**). However, this deformation was already determined when designing or manufacturing them. Therefore, the desirable properties of future programmable and responsive mechanical metamaterials should have local activation of property changing and programmability of deformed structure to displaying more dynamic deformation.

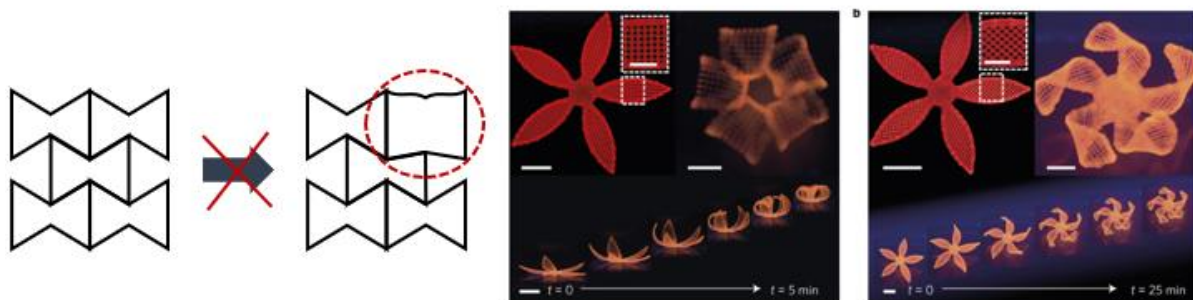


**Figure 8** Two limitations of formal programmable metamaterials: 1) the lack of local property change,

2) showing only pre-determined actuation or shape changing.

From the question of whether it is possible to change Poisson's ratio from negative to positive, I have compared the negative Poisson's ratio and positive Poisson's ratio honeycomb structure. When examining the re-entrant honeycomb structure, the part that was bent was stretched to enlarge the inclusion area of the structure and then showing negative Poisson's ratio behavior. Thus, from this, I assumed that we could switch the Poisson's ratio from negative to positive through changing the stiffness of the part that will undergo deformation<sup>21</sup> (Figure 9).

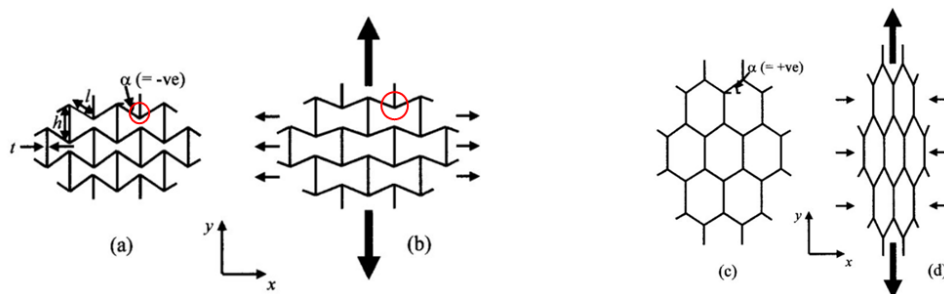


**Figure 9** If we can morph the stiffness of the local parts where the shape change most largely occurs, we could change the Poisson's ratio of the structure.

### Design & Expectation

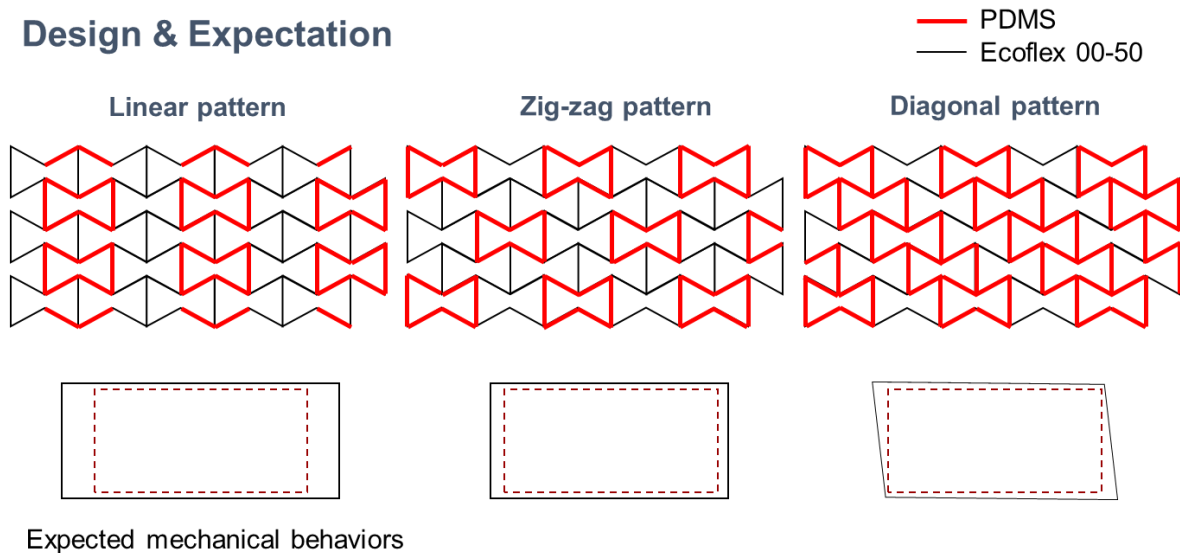


**Figure 10** The three patterns designed with two silicone rubber which have different stiffness.

From that idea, I designed three patterns of the re-entrant honeycomb structures with two silicone rubber

with different stiffness (**Figure 10**). Since the Polydimethylsiloxane (PDMS) is rigid than the Ecoflex 00-30 part, I expect that the part made of PDMS would not deform as much as the Ecoflex part so that deformed in the different shapes depending on the patterns. Three patterns were named linear, zig-zag, and diagonal patterns. The expected mechanical behaviors of each structure were shown in figure 10. In expectation, the linear pattern would be stretched the most because it has more compliant Ecoflex columns in the structure and the zig-zag pattern will not stretch much due to the stiff PDMS unit are sparsely located. Lastly, for the diagonal pattern, I expected that this structure will be deformed in a parallelogram shape.

The structures were made with mold that printed from a 3D printer. PDMS part was poured and cured, then cut into the desired shape. After removing the unnecessary part from the mold, Ecoflex was poured into the last part of the mold and cured. The structures were stretched to see if the mechanical behavior of metamaterials is matched with the expectation. In the real experiment, three patterns did not show a big difference when stretched. This limitation might arise from the fact that there is no large difference in stiffness between PDMS and Ecoflex. This experiment reminds me of the necessity of larger differences in stiffness (**Figure 11**).

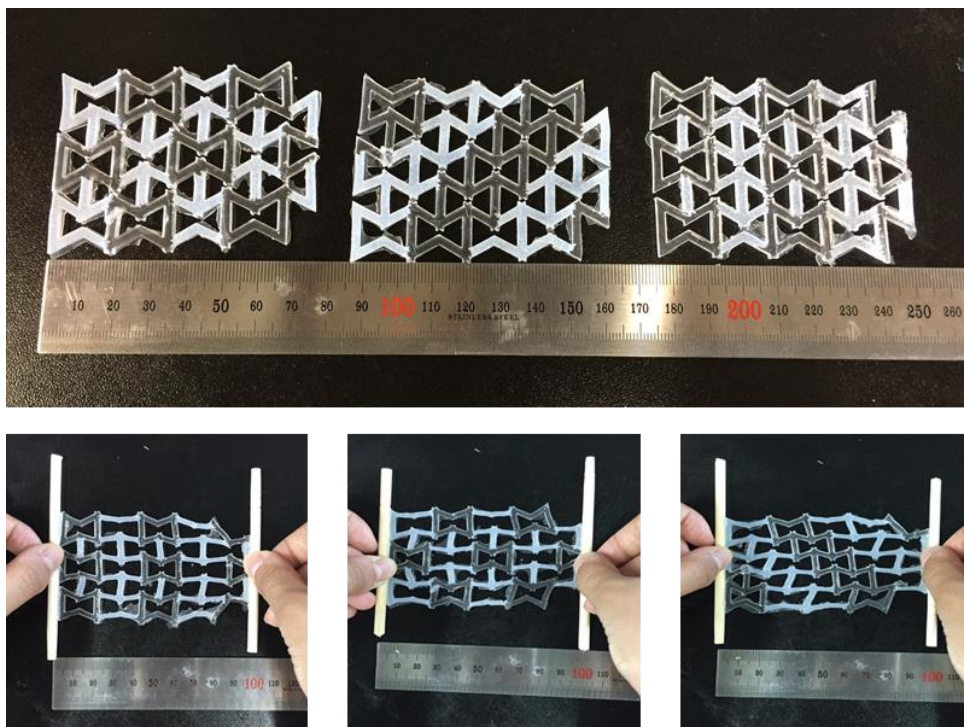


**Figure 11** In reality, there were no big different deformation in the three patterned structure, since the stiffness difference of two silicone rubber were not as big as showing distinctive change in Poisson's ratio.

### 1.3. Stiffness changing smart materials

The alternative materials that I chose for larger stiffness difference with soft silicone rubber were the Low Melting Point Alloy (LMPA). LMPAs are metal that has a relatively low melting point such as 47 or 62°C, thus can be used as stiffness changing element (from hard to compliant, or compliant to hard) in metamaterial structure through the easy phase transition. Also, if LMPA is embedded in the compliant metamaterial structure, the shape of the materials can be fixed when LMPA is in solid-state and reconfigurable when LMPA is in liquid-state. There are already existing studies that embedding LMPA in soft silicone rubber structure, such as variable stiffness soft gripper and actuator (**Figure 12**). Field's metal, which has a melting point of 62°C, was used in the usual case of these studies.

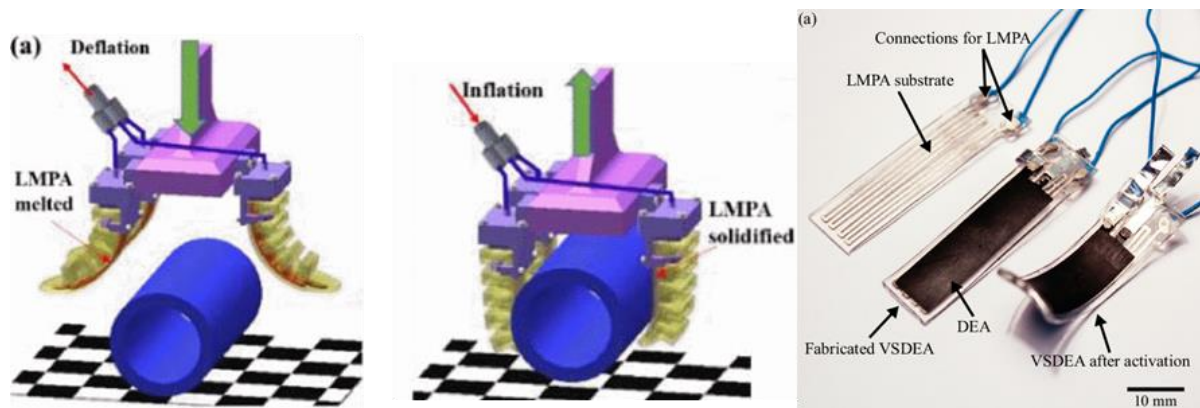


**Figure 12** The stiffness changing soft gripper and actuator through embedding LMPA in the structures<sup>22,23</sup>.

I have embedded LMPA into a re-entrant honeycomb structure and graphene-based carbon foam structure. Firstly, I have made groves in the beam of silicone rubber re-entrant honeycomb structure. Embedding the LMPA into the grove and sealing it was successful, however, it was found out that there was a lack of local controllability of stiffness. Since embedded LMPA was linked over many units in the re-entrant structure, it was impossible to control the single units in the structure (**Figure 13**). The graphene-based structure is originally showing buckling when this structure is compressed through bending the beams. I embedded LMPA in the four beams in structure to functionalize the structure. I expected that the structure will make buckling under compression when the LMPA layer is in a liquid state, exhibiting negative Poisson's ratio, and prevent buckling when the LMPA layer is in solid-state, showing positive Poisson's ratio. However, it turned out that the difference of stiffness between liquid LMPA and silicone rubber hindered the buckling of LMPA embedded beams. Therefore, the experiments of embedding LMPA in these two structures were ended up in failure.

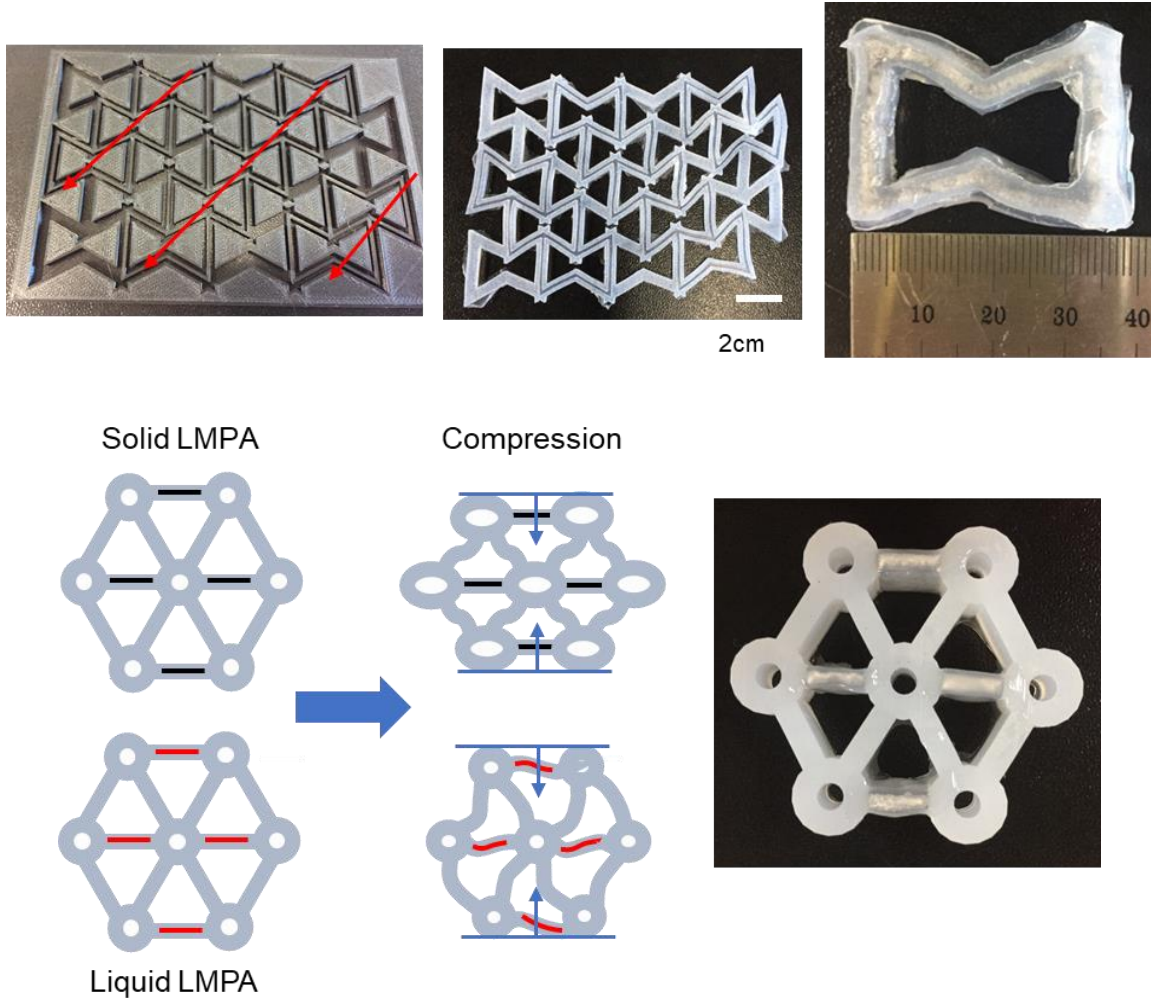


**Figure 13** I embedded LMPA in the two negative Poisson's structures; re-entrant honeycomb structure and graphene-based structure. Embedding the LMPA layer in each structure was successful, however, the former structure was lack of local control of stiffness, and the latter structure did not deform as I expected.

After the failure, I have come to search for other structures for assigning local control of stiffness and better performance. The new structure that I chose was a structure of the periodic arrangement of voids. Advantages of using this structure are that it is easy to assign engineered property for a single, separated unit. For example, in case of re-entrant honeycomb structure, one beam in the structure is belong to two units. Also, periodic void array is having simple shape of units compare to other negative Poisson's ratio metamaterials so that it will allow easier manufacture of engineered structures such as handling LMPA layer.

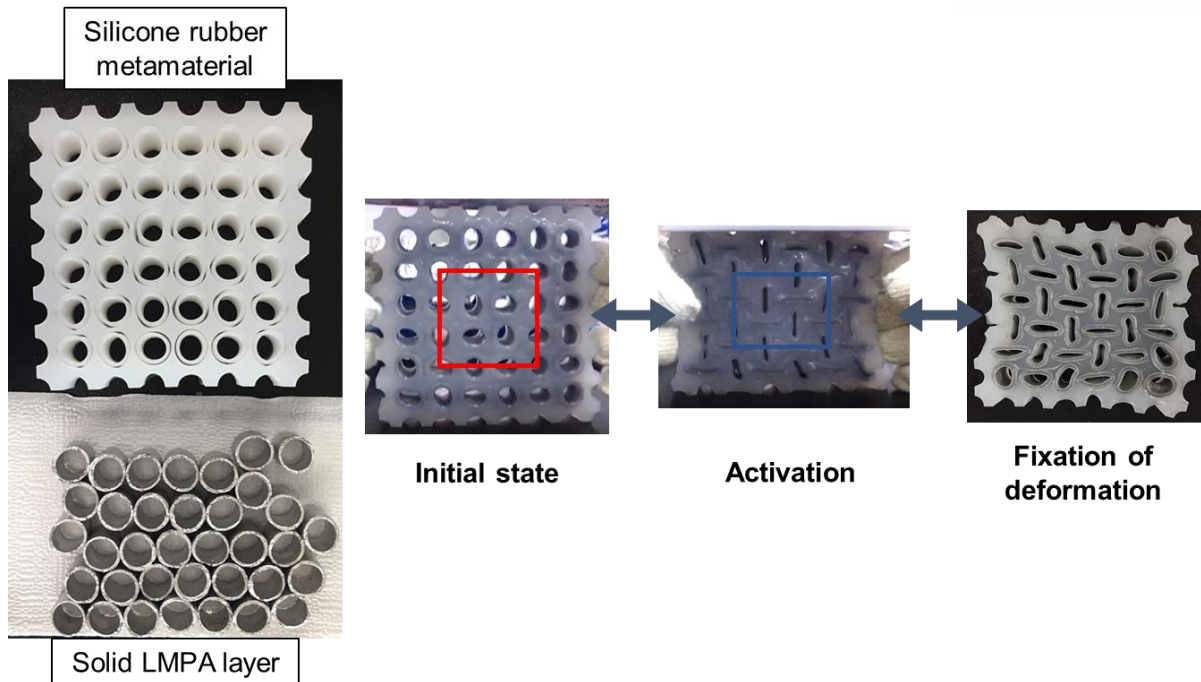


**Figure 14** Cylindrical LMPA layers were put into groove near periodic voids and sealed. This periodic void structure changes its stiffness depending on the temperature. However, this structure still lacks the local programmability.

The LMPA parts were embedded in the groves near the boundaries of the voids. Solid LMPA layers were prepared with another silicone rubber mold made by the pre-mold that printed with 3D printer (Ultimaker 2), then they were sealed with same silicone rubber that was used for body of the structure (**Figure 14**). In the initial state, the structure does not deform by the applied pressure due to the stiffness of the solid LMPA layer which resist the deformation of the voids. When the metamaterial is activated by heating the structure, the material was showing abrupt instability under compression and making buckling since every LMPA layer is in liquid state so that voids are compliant. Moreover, I could fix the deformed shape by cooling down the structure while maintaining the applied pressure. However, the metamaterial could be activated through applied heat to ‘entire’ structure. Therefore, I began to think of local control for each void, and consider each void as a single activation unit, mechanical pixel.



#### **1.4. Mechanical metamaterial with pixelated activation units**

Local activation to change the material's property will endow mechanical metamaterials' dynamic deformations and enhanced resolution of controllability. To enable the separate activation of stiffness changing elements, we applied the electrical interface to the mechanical metamaterial. For separate activation, I designed separate heating layers located near the stiffness changing units (LMPA layers). These heating layers are activated through applying voltages (Joule heating) directly to the only desired mechanical pixel.

The goal of this thesis is to develop a new mechanical metamaterial system with higher controllability and programmability and showing diverse patterned deformations. From the pixelated metamaterial's dynamic and responsive features, I anticipate that this metamaterial will develop into more sophisticated soft material systems, and give inspiration to other's work. This metamaterial might be used in wearable devices, or stiffness changing soft robotics.

#### **1.5. Outline of the thesis**

In Chapter 1, this thesis is describing the definition of mechanical metamaterials and examples of subcategories of mechanical metamaterials. Stiffness changing elements embedded in several mechanical metamaterial structures and the limitations of them were introduced, followed by the necessity of pixelated activation was discussed. In Chapter 2, the pixelated mechanical metamaterial structure and fabrication method will be explained. The characteristics of composites and layers were analyzed. Chapter 3 propose the activation and actuation cycle of pixelated mechanical metamaterials of the entire structure and single mechanical pixel. Chapter 4 discusses Poisson's ratio of the mechanical metamaterial and compare this with silicone rubber structure. Chapter 5 is the summary of the thesis, strengths and limitations, and future work of this research.

## CHAPTER 2 Fabrication methods & materials

This chapter describes the structure of the pixelated mechanical metamaterial, mold preparation, fabrication method of the structure, and characteristics of each layer.

### 2.1. Structure of pixelated mechanical metamaterials

The pixelated mechanical metamaterial comprised of three distinct layers, and it contains seven by seven periodic voids array, which voids' shapes are elliptical. Thus, the shape of the structure is one of the representative auxetic structure that shows negative Poisson's ration under the uniaxial compression by buckling. Those voids which are located in the nearest point are placed perpendicular to each other. Voids in the structure are named as a pixel, since each void function as a controllable functional unit, and can be operated separately. The whole size of the structure is 96mm x 96mm x 35mm (width x length x height), and the major and minor axis of voids are 0.88mm and 0.8mm (porosity of the structure: 0.384). The three layers that are composing the pixelated mechanical metamaterial are the conductive heating layer, phase-transition layer, and silicone rubber layer. The cylindrical-shaped voids in the structure are made up of the conductive heating layer, meaning that the conductive heating layers are located at the boundaries of each void, and the phase-transition layers are embedded between the conductive heating layer and the silicone rubber layer. The silicone rubber layer wraps up other layers and forming the whole structure. The conductive heating layer is also comprised of silicone rubber but containing the nine wt.% of superconductive carbon black to serve the function of Joule heating. Two lead wires are embedded in the conductive heating layer, which is placed at the end of both the minor axis of each void and the wires function as electric wires in the electrically controllable system. The phase-transition layer changes its stiffness by heating so that this layer can activate and deactivate each pixel according to the phase of the layer. This layer is made of Low Melting Point Alloy (LMPA), which melting point is 61 °C. When the phase-transition layer is in a liquid state due to the electrical stimulus, the relevant void of that layer can be deformed by the external pressure. The state that the conductive heating layer is electrically on, and the phase-transition layer is in the liquid state is called activation of the void. However, when the phase-transition layer is in the solid-state, the layer maintains its stiffness even when the uniaxial compression is applied to the structure. The pixelated activation of the structure has its advantages that we can select the desired voids to activate, and the structure can show a variety of pattern deformation.

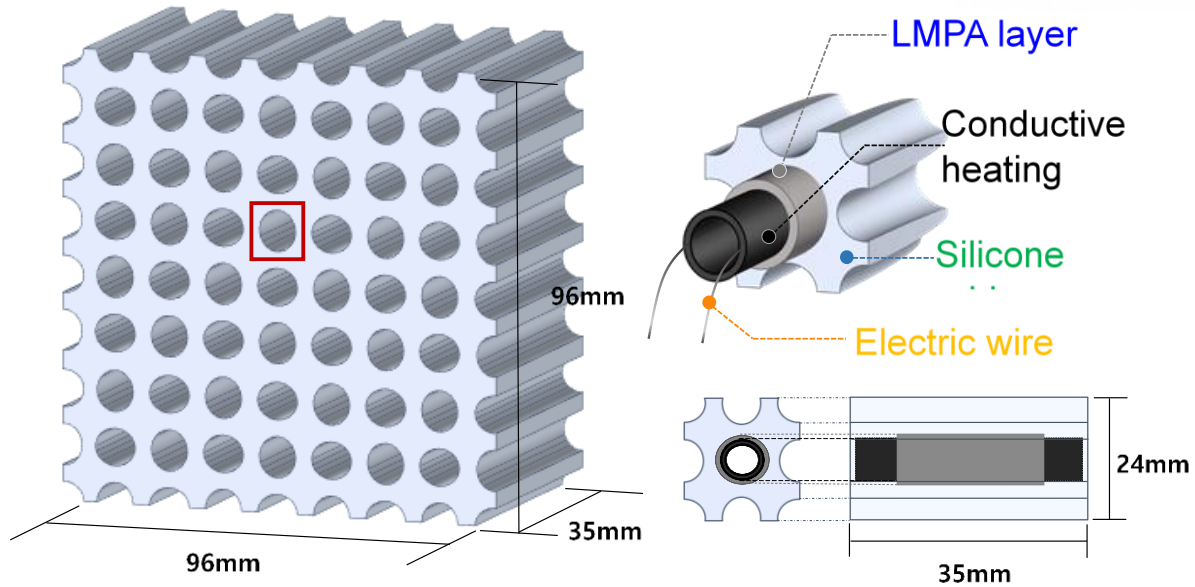


**Figure 15** The figure of the pixelated programmable mechanical metamaterial. This engineered metamaterial is comprised of three layers which are a conductive heating layer, LMPA layer, and silicone rubber layer. The electric wires are embedded in the conductive heating layer to apply electric stimuli to the structure to induce the phase transition of the LMPA layer.

## 2.2. Mold design & printing

A total of three kinds of molds or structures are required for the fabrication of pixelated mechanical metamaterials; 1) mold for silicone rubber layer, 2) pillars for the conductive heating layer, and 3) pre-mold of the LMPA layer. The design of the molds and pillars are prepared by the 3ds Max program, considering the real-size of the metamaterials, and the molds and pillars are printed on a 3D Printer (Ultimaker 2).

### 2.2.1. Mold for silicone rubber layer

The mold for the silicone rubber layer is designed for use at the last step of fabricating the mechanical metamaterial. This mold has printed in two-part and assembled when using for fabrication. The first part of the mold is a box-shaped mold with an inside outline of the mechanical metamaterial structure, with seven by seven periodic elliptical holes, which are exactly the same as the void array in the metamaterial, on the bottom of the mold. Those holes are designed to insert and fix the pillars to make cylindrical voids in the final structure. The size of the structure is 125mm x 125mm x 37mm, and it is printed with polyvinyl alcohol (PVA) filament, which melts in water. The other part of the mold's shape

is a cuboid with seven by seven periodic holes of about 20mm deep to hold 49 pillars, and also printed with PVA filament. This mold placed under the box-shaped mold, and it has a role to fix inserted elliptical pillars. The size of the mold is 140mm x 140mm x 25mm.

### **2.2.2. Pillars for the conductive heating layer**

A total of 49 pillars are printed to make void arrays through inserted in the molds for silicone rubber. They are a cylindrical shape with elliptical bottoms and have a scale of 0.88mm x 0.8mm x 60mm (major axis x minor axis x height). These pillars are used to fix the conductive heating layers' location in the structure of the mechanical metamaterial.

### **2.2.3. Pre-mold and mold for the LMPA layer**

Before handling the LMPA layer, the mold of the layer is prepared by two steps. Pre-mold for the LMPA layer is necessary because the mold of the layer is fabricated with silicone rubber, which requires pre-mold. Thus, pre-mold was printed by the 3D printer with the PVA filament, then liquid silicone rubber was poured into the pre-mold. It was cured for one hour on a hotplate at 80°C for polymerization. Pre-mold was removed from the silicone rubber mold after it's solidification.

## **2.3. Fabrication of functional layers**

To fabricate the pixelated mechanical metamaterial, it involves several steps of preparation of functional layers. Conductive heating layers and phase-transition layers should be fabricated before the assembly of each layer, by enclosing them with silicone rubber.

### **2.3.1. Fabrication of conductive heating layer**

Ecoflex 00-30(Smooth-on Inc.), and Carbon Black(Super P, Alfa Aesar) were mixed in the weight ratio of 100:9 under the room temperature to make conductive sludge. Lead wires were prepared ahead of making the conductive sludge to embedded in the conductive heating layer. Five thin lead lines were twisted into a single wire, and a total of 98 lead wires were produced. The sludge was applied on a flat aluminum foil, and it was spread into a 0.25mm thickness layer through a micrometer adjustable film applicator. Two lead wires were put across in the middle of the sludge with keeping a distance of 13mm apart from each other and fixed with sticky tape. The sludge was applied again on the fixed wires and spread into a layer with a thickness of 0.6mm with the micrometer adjustable film applicator (**Figure**

16). Then the sludge layer was placed on a hotplate at 80°C for boosting the speed of polymerization of silicone rubber sludge for five minutes. The polymerized layer was cut into a rectangular layer with a size of 34mm x 30mm. A total of 49 number of conductive heating layers were prepared by repeating the process.

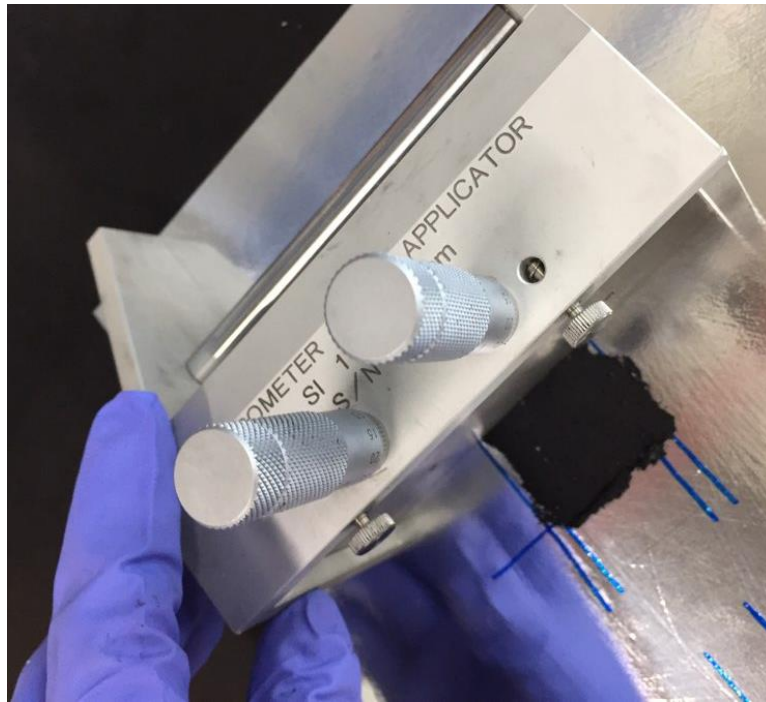


**Figure 16** The sludge of the conductive heating layer is spread by the film applicator at a thickness of 0.25mm. Then the electric wires are fixed on the spread sludge, and they are covered with additional sludge. After that, the additional sludge was spread at a thickness of 0.6mm.

### 2.3.2. Fabrication of phase-transition layer

Field's metal was selected to fabricate the phase-transition layer, and the solid LMPA was put on a hotplate at 130 °C for 30 minutes to melt into liquid completely. The silicone rubber mold of the phase-transition layer was also put on the hotplate for ten minutes before the injection of LMPA into the mold to keep LMPA in a liquid state while injecting it into the mold. The liquid LMPA was injected into the ring-shaped void of the mold with a syringe. The mold was placed on the hotplate during injection to prevent the solidification of LMPA. After injecting the LMPA, the mold was soaked in water at room temperature to solidify. The fabricated phase-transition layer is a hollow elliptic cylinder shape with a major axis of 1.04mm and a minor axis of 0.96mm, a thickness of 0.4mm, and a height of 15mm.



**Figure 17** Field's metal was melted on the hot plate with a temperature of 130°C for 30 minutes. Liquid LMPA was then poured into the silicone mold to fabricate the cylindrical LMPA layer.

## 2.4. Assembly of layers

### 2.4.1. Attachment of the conductive heating layer on the pillar

Since each layer was separately prepared, the layers should be assembled to complete the production of the pixelated mechanical metamaterial. The following steps are required to put together the readied conductive heating and phase-transition layers. The Eco-flex 0030 was mixed again with Carbon Black with a nine weight percent, and the sludge was spread thinly on the conductive heating layer. The layer wrapped around the upper part of the printed pillar, leaving about three centimeters behind to insert the pillar into the mold for the silicone rubber layer. When wrapping up the pillar, the lead wires embedded in the conductive heating layers were placed diametrically on the minor axis of the elliptical shape pillar. The wrapped pillars were put on a hotplate at 80 °C for 5 minutes to polymerize the applied sludge for complete attachment of the conductive heating layer to the pillar. As a result, 49 pillars are wrapped with conductive heating layers (**Figure 18**).

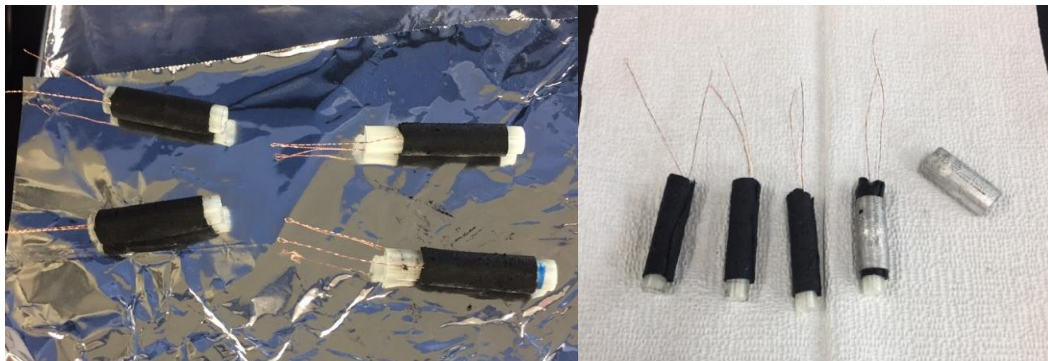


**Figure 18** The pillars made of PVA are wrapped with conductive heating layers, and they were fixed with conductive heating layer sludge on the hotplate. Cylindrical LMPA layers were wrapped around the conductive heating layer by applying the silicone rubber adhesive on the surface of the heating layers and the inside of the LMPA layers.

### 2.4.2. Putting together the LMPA layer and the pillar

Silicone adhesive (Sil-Poxy, Smooth-On) was applied inside the cavity of the pre-made phase-transition layer and on the surface of the conductive heating layer wrapping around the pillar. As the major and minor axis of the phase-transition layer's cavity is a bit larger than the diameter of the wrapped pillar, the wrapped pillar was inserted in the cavity of the LMPA layer. The LMPA layer was placed in the middle of the area of the conductive heating layer because to make sure that the LMPA layer should be located in the center part of the metamaterial's height. Total 49 PVA pillars were wrapped with the conductive heating layer and the phase-transition layer.

### 2.4.3. Silicone rubber layer

Assembled pillars were put into the cavities of the box-shaped and cuboid-shaped silicone rubber molds. After inserting 49 pillars into the holes of structural mold, silicone rubber was poured into the remaining part of the mold to encapsulate the pillars and the other layers (**Figure 19**). Then the molds were placed into the vacuum chamber to degassing for 25 minutes and cured on a hotplate at 65 °C for one hour. PVA pillars and the silicone rubber mold were removed by submerging the structure in the water for 1 to 2 days. After removing the pillars and the mold, the pixelated mechanical metamaterials has 49 periodic voids array and contains the phase-transition layer and the conductive heating layer inside each void of the structure.



**Figure 19** Liquid silicone rubber was poured into the mold after putting all pillars into the cavities in the bottom of the mold. To remove air bubbles, the mold was placed in the vacuum chamber for 25 minutes. After degassing, the mold was placed on the hot plate at 65 °C for one hour to cure the silicone rubber.



#### 2.4.4. Arrangement of electric wires

Two electric wires are embedded in each of the voids in the metamaterial, and one of the wires from the same row of the voids are connected in the lateral direction. The other wire from the same column of the voids is connected in the perpendicular direction. The seven connected wires are in each lateral and vertical direction of the metamaterial, and a total of 14 connected wires are produced (**Figure 20**).

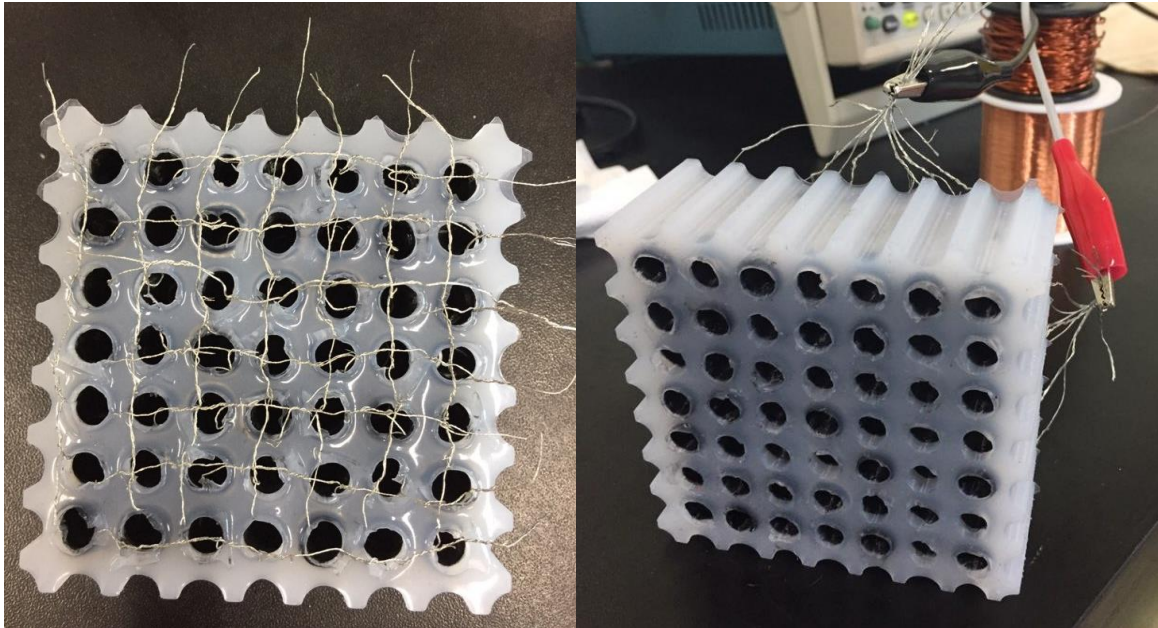


**Figure 20** Electric wires are arranged in two directions – vertical direction and lateral direction.

### 2.5. Characterization of functional layers

#### 2.5.1. The electrical conductivity of the conductive heating layer

The electrical conductivity of the conductive heating layer matters to operate the metamaterial effectively, and it affects the Joule heating during the activation. Thus, the electrical conductivity of the conductive layer was measured according to the concentration of the Carbon Black dispersed in the layer (**Figure 21**). The range of the concentration of the Carbon Black of the measured layer was 1.0 wt.% to 10.0 wt.%, at an interval of 1.0 wt.%. The electrical conductivity was calculated as  $\sigma=L/AR$  by measuring the resistance of a layer with the size 34mm x 30mm x 0.6mm (width x length x thickness), where A and L are the area and length of the layer. The resistance was measured with the True RMS Multimeter (Fluke). Almost no electrical conductivity was estimated at a low concentration (1.0 to 3.0 wt. %) of Carbon Black since the insufficient Carbon Black networks in the composite. From 4.0 wt.% to 6.0 wt.%, the calculated electrical conductivity was drastically increased in  $10^5$ -fold. About at a 6.0

wt.% of Carbon Black concentration, the concentration might be the percolation threshold, where the conductive networks are well-formed in the composites. Electrical conductivity gradually rises even after passing the concentration of 6.0 wt.%, and the concentration of 9.0 wt.% was selected for the conductive heating layer because it was the highest Carbon Black concentration that can be fabricated without the difficulty of mixing. From the concentration of 10.0 wt.%, the sludge of the composite becomes too stiff to mix. The electrical conductivity approaches  $2.04 \text{ S}\cdot\text{m}^{-1}$  at a Carbon Black concentration of 9.0 wt.%.

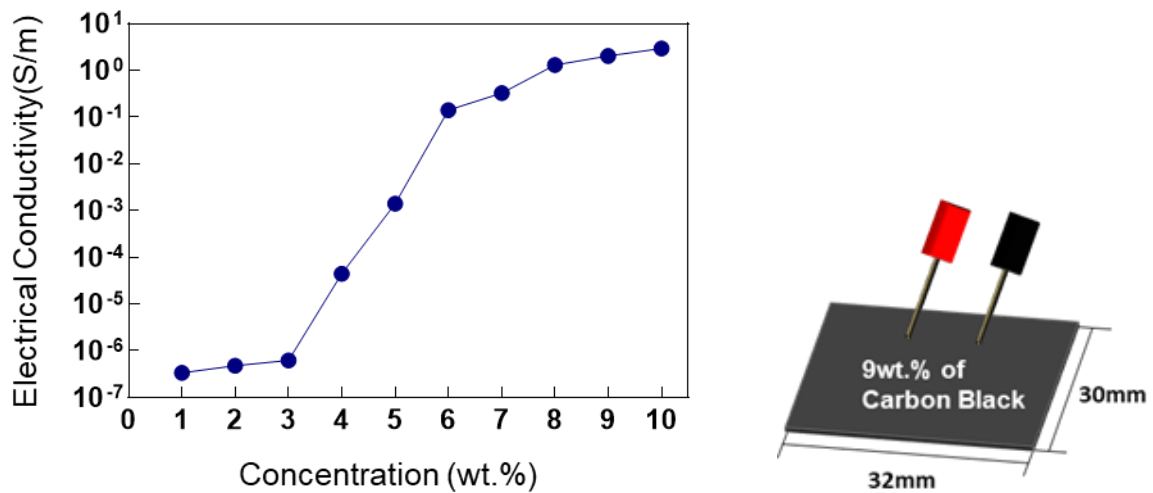


**Figure 21** The electrical conductivity was measured according to the concentration of carbon black (wt. %) from 1 to 10 wt.%.

### 2.5.2. The electrical resistance corresponding to the connected number of voids

The electrical resistance of the pixelated mechanical metamaterial according to the connected number of voids was measured by the True RMS Multimeter (Fluke). This resistance system is based on the parallel connection of every void in the structure. The resistance of one to seven connected voids and one to seven rows of voids were measured, and the values were compared with the numerical value of the resistance according to the number of connected voids from the parallel resistor equation. The experimental values and the numerical values were almost the same so that the system accords with the parallel connection of resistance. Therefore, the metamaterial system can be operated with the proper voltage application since the system follows the law of the parallel connection of resistance (**Figure 22**).

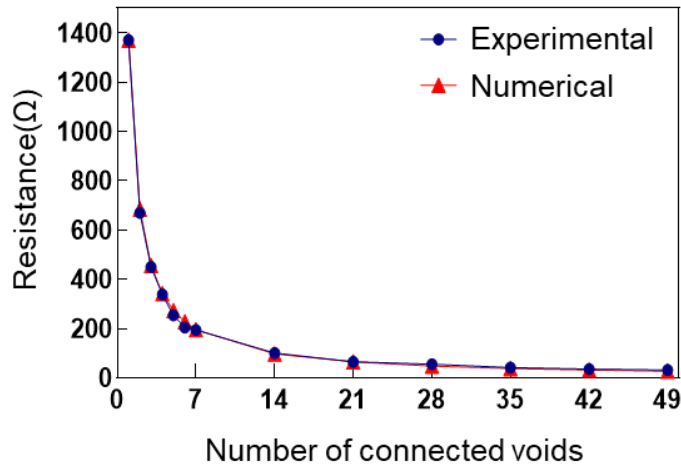


**Figure 22** The resistance of the structure was measured according to the connected number of voids and compared with numerical value.

### 2.5.3. Repetitive operation of the system and the temperature profiles

The voids of the metamaterial can be activated by applying the electrical stimulus. To compare the activation, which differs from the applied voltages, the temperature of the single void was tracked. All of the voids in the structure were turned on and off three times for 2400 seconds to exhibit the repetitive activation, with three periods of on and off the structure. The time that takes for heating and cooling of the single void was also tracked by putting in a thermometer in a single void, and record videos during the process then trailed the temperature every ten seconds. These procedures were repeated with different applied voltages of 25V, 22.5V, 20V, 15V, and 10V. For the first heating period (0 to 400 seconds), the maximum temperatures of the heating layer were 91°C and 78 °C, which are above the melting point of the phase-transition layers, at voltages of 25V and 22.5V respectively. Yet, the applied voltages that are lower than the previous one could not be able to raise the temperature of the heating layer to the melting point of the LMPA layer. For 20V, 15V, and 10V, the maximum temperatures of the layer were 51.8 °C, 41 °C, and 29.1 °C during the first heating cycle. The changes in the maximum temperatures during three periods of turning on and off the structure were tracked, and the maximum temperatures were almost maintained. Thus, the structure was able to do activation repetitively as well as the temperature of the heating layer drastically increased in about the first 200 seconds of activation and cooled down until solidifying the LMPA layer in about 200 seconds. Therefore, the engineered metamaterial can be activated and deactivated the selected domain repetitively within a short period (Figure 23).

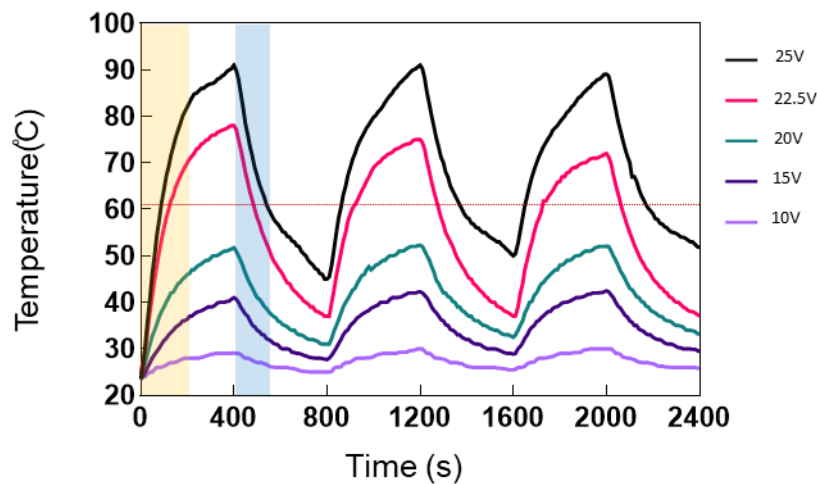


**Figure 23** The temperature of a single void was tracked during 2400 seconds with turning on and off the structure three times. Applied voltages were range from 10V to 25V.

#### 2.5.4. Heat transfer of the system

The heat transfer is a significant issue to take into account since the possibility of temperature influences from nearby voids. The temperature changes in four deactivated adjacent voids of a single activated void were tracked for 600 seconds to demonstrate the little effect of the heat transfer in the structure. The temperature of the void approached to 71°C in 600 seconds when 25V was applied. The location of the four adjacent deactivated voids is the nearest void, the second nearest void, diagonally nearest void, and diagonally second nearest void. The nearest void's temperature raised to 43 °C, which was the highest temperature among four adjacent voids at the end of the heating time. The second nearest void's temperature was higher than the diagonally nearest void's temperature at 600s. The diagonally second nearest void almost does not affect by the temperature of the activated void. All of the adjacent voids' temperature fails to reach the melting point of the LMPA layer so that the activation of metamaterial is locally programmable without affecting the deactivated domain (**Figure 24**).

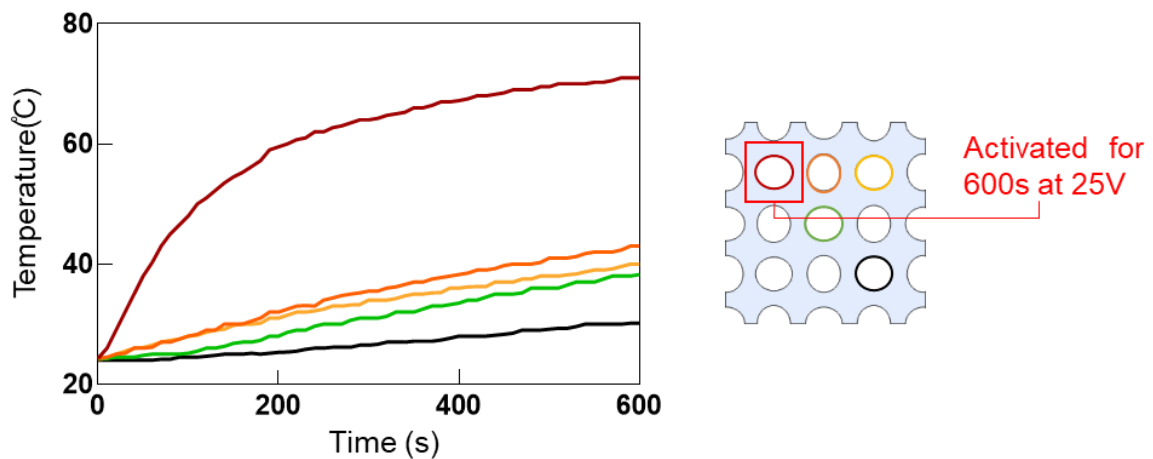


**Figure 24** Temperature change of the voids near the activated void were tracked for 600 seconds.

## CHAPTER 3 Activation & actuation of the pixelated mechanical metamaterial

This chapter represents the operation cycle of the metamaterials, domain activation and actuation of the structure, and fixation of the structure.

### 3.1. Operation Cycle

The pixelated mechanical metamaterial activates through the electric stimulus and actuates through uniaxial compression. Since the activation is programmable and reversible, it is possible to exhibit a variety of patterned activation and actuation.

#### 3.1.1. Operation setting

The seven rows and the seven columns of connected wires are stemmed from each conductive heating layer. For a single void, one of the wires is connected to a row of wire, and the other one is connected to a column of wire. Thus, the voids of the cross-section point of the selected rows and columns of wires would be activated when the electric stimulus is applied. By choosing the diverse combination of rows and columns of wires, we can show a wide range of patterned deformation of the structure (**Figure 25**). When the pattern of voids for activation is chosen, the voltage is applied to the lateral and perpendicular direction of wires through DC power supply (Tektronix, PWS2326). The voids became compliant by the Joule heating of the conductive heating layers so that the phase-transition layer changed into a liquid phase.



**Figure 25** DC power supply was used for applying an electric stimulus to the pixelated mechanical metamaterial.

### 3.1.2. Activation of a single unit

The single void's activation is achieved by the application of voltage on the corresponding void. Even though two wires from the same void are connected to lateral and perpendicular directions, each pixel can be individually controlled by separating them from the connected wires. The phase-transition of the LMPA layer follows by the application of the voltage to wires, and the void is prepared to be deformed by external pressure. Both activation and the deformation of the voids are reversible, as well as deactivation of the voids rigidifies the voids again and maintain the structure's rigidity. The compliant void can gain rigidity again with the deformed shape or turn back to its original undeformed shape, depending on the existence of uniaxial compression. The shape fixed void due to the rigidity can turn back to the initial state by activating it again (**Figure 26**).

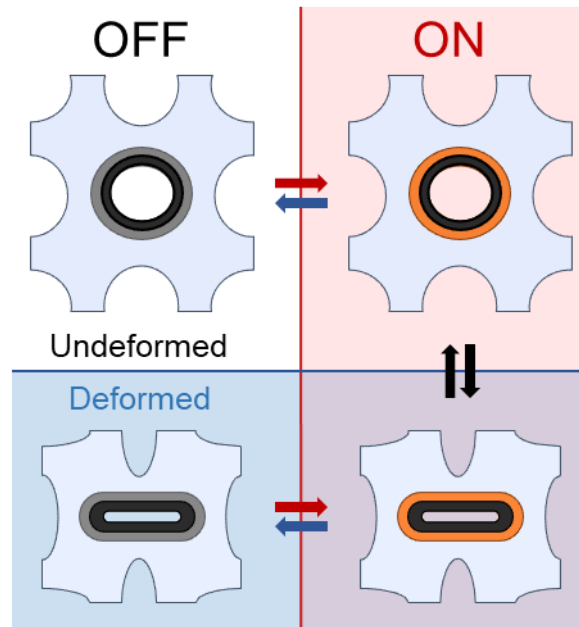


**Figure 26** This is the figure of the local activation of a single void. Through an electrical and mechanical activation, the single pixel is deformed and fix its' shape.

### 3.1.3. Operation cycle

The whole structure of pixelated mechanical metamaterial is locally programmable and re-deformable in the process of activating and deactivating the voids. In the initial state, the metamaterial has rigid phase-transition layers as the LMPA is in solid-state, maintaining the stiffness of the structure. Since LMPA layers are solid and deactivated, it is difficult to deform voids to induce buckling, and the metamaterial does not display auxetic behavior. To activate the desired domains, the voids of the domain should be selected and activated through Joule heating. The heated voids become compliant due to the melting of the LMPA layer and make buckling under pressure. However, only the domain of selected voids represents auxetic behavior, and the rest of the domain stays rigid. This deformation is reconfigurable *in situ*, during the activation of the metamaterial, as well as the pixelated control of activation, which is possible. The structure can turn back to its initial states by deactivating and removing the applied pressure. It can also fix the deformed shape of the structure by deactivating the domain while maintaining the buckling state under pressure. When the deformed domain is cooled down under the external vertical pressure, the LMPA layer is solidified with deformed shape. Yet, we can restore its original state by activating the deformed domain again. When the electric stimulus is applied again, deformed phase-transition layers meltdown and the corresponding voids recover to their initial shape. The entire process was reversible, and it showed the programmability of the system with pixelated control of voids through changing the stiffness (**Figure 27**).



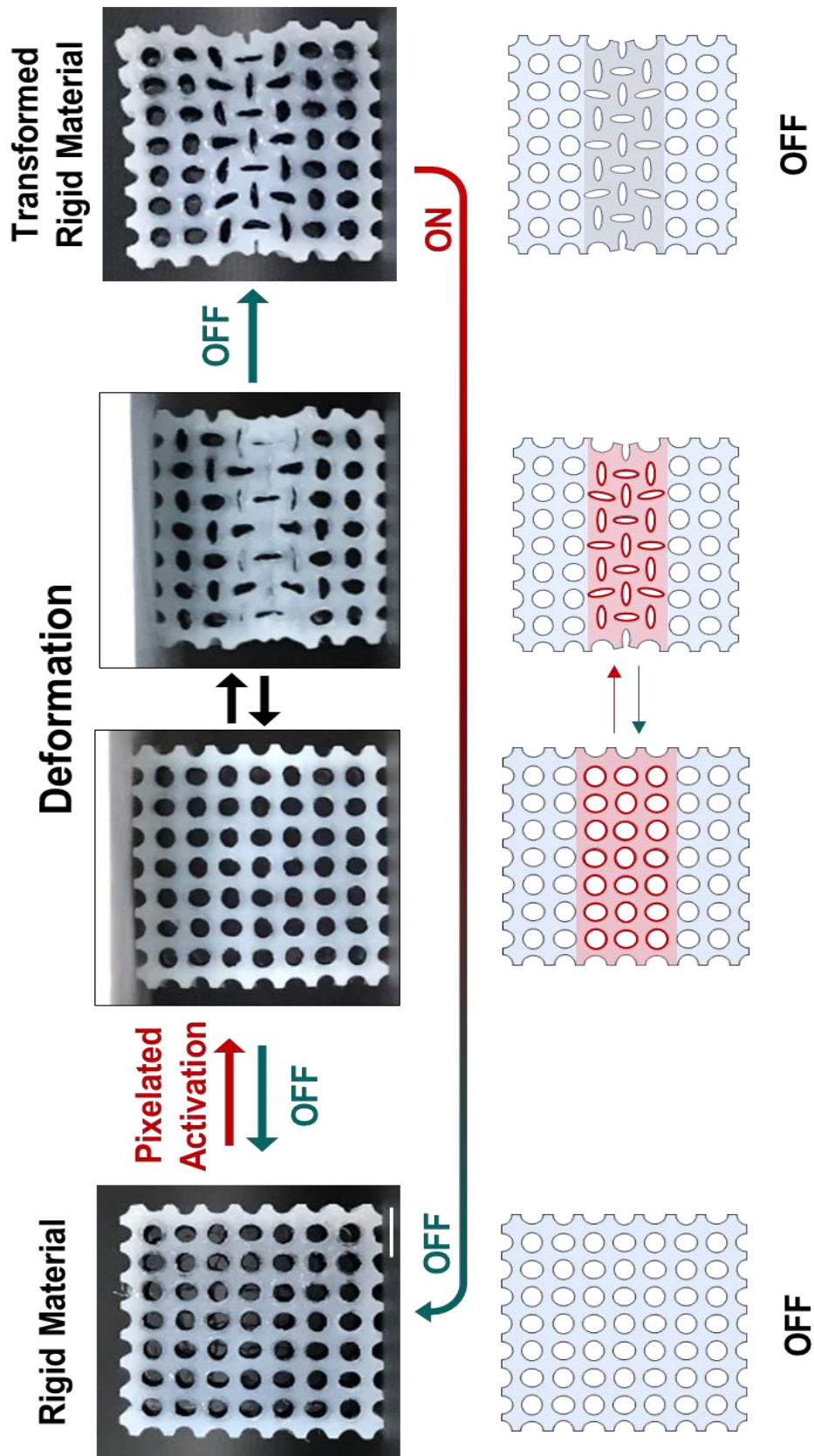
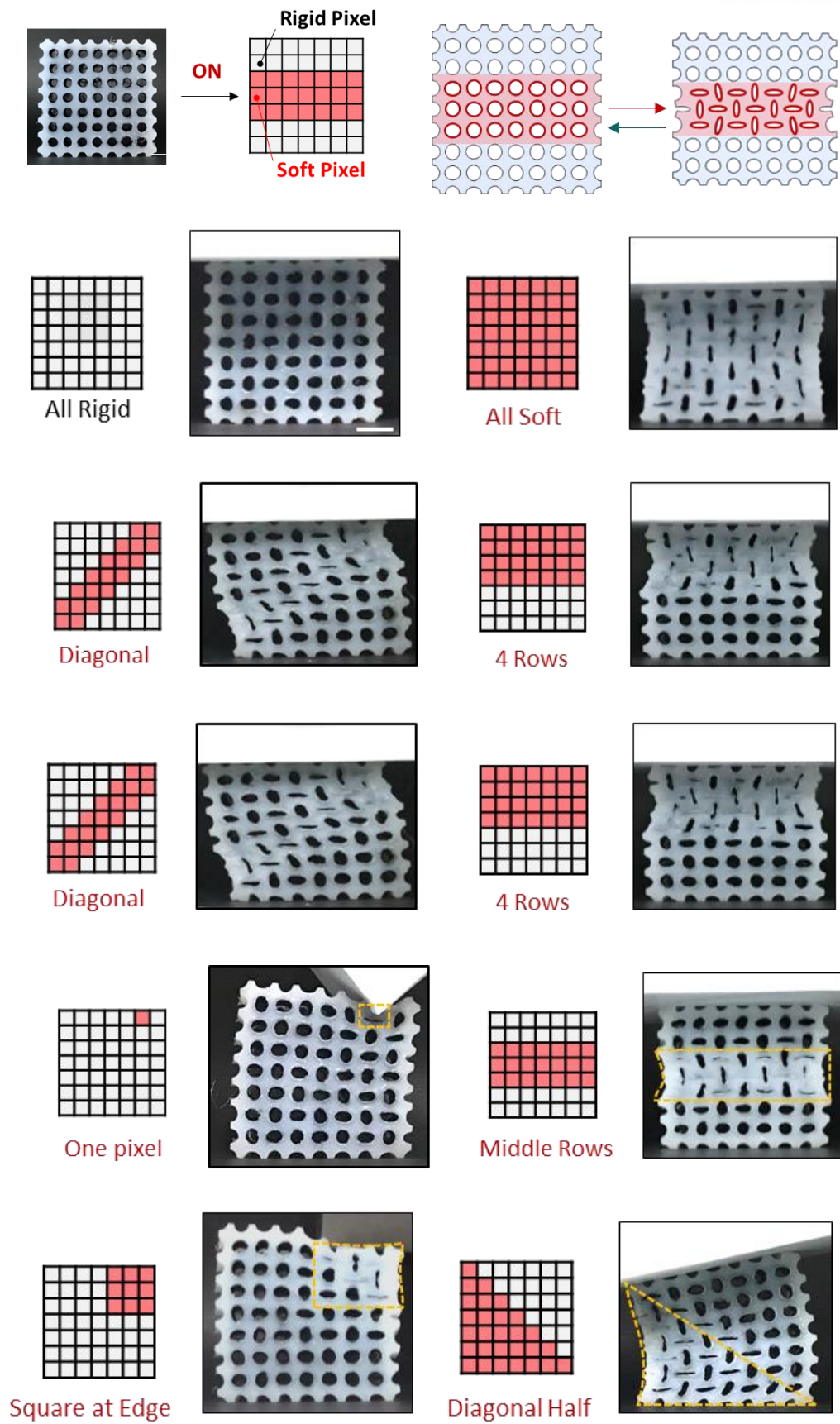


Figure 27 The whole cycle of pixelated activation of the mechanical metamaterial.

### 3.2. Diverse domain deformation of metamaterial

Depending on where the electric stimulus does has applied, the structure can show varied patterned activation and deformation. With this patterned activation, rigid pixels and soft pixels are coexisting. The patterned deformation is transient in that the metamaterial easily restores the initial configuration by removing the uniaxial compression. Ten patterns were selected to show pixelated control of voids; 1) All rigid, 2) all soft, 3) diagonal, 4) four rows from the top, 5) a middle row, 6) all pixels except the three by three edge, 7) three by three at the edge, 8) diagonal half, 9) one pixel at the boundary, and 10) three rows in the center of the structure (**Figure 28**). The patterned activation induces the formation of the domain boundaries under pressure. 1) without activation, the whole metamaterial maintains its' stiffness and cannot be deformed under compression. 2) When every void in the metamaterial is activated, the structure represents negative Poisson's ratio behavior with buckling over the single domain. 3) three rows of the diagonal direction have activated and pressed with shear stress. The activated part separates both sides of the corner of the structure so that it exhibits three-domains. 4) Uniaxial loading is applied to the structure with activating the four rows from the top, and it showed a two-domains structure with a horizontal boundary. 5) The shear pressure was applied to the metamaterial after activation of a single row in the center to make a deformation. The deformed middle row does not show the auxetic behavior but switched the shapes into synchronized buckling. The deformed row functions as a domain boundary, thus the upper domain of the metamaterial is pushed to the shear direction. 6) The voids except three by three at the edge were activated, and the shear compression was applied to the activated domain. Only the activated voids were buckled, and the deactivated domain was distinctive. 7) Three by three corner voids are selectively compressed, confined to the activated corner domain, and the buckling region was noticeable to show a two-domain structure. 8) To making deformation of the bottom diagonally half of voids, the compression was applied to the structure in a tilted direction. Only activated local domain has deformed. 9) A single activated void at the boundary of the structure displays the void deformation in the direction of the compression. 10) When three rows of the voids in the center are compressed in the vertical direction, it makes a three-domain structure with two horizontal domain boundaries through induced buckling in the middle. The pixelated activation enables varied selective buckling behavior from the pre-designed structure of the metamaterial with re-programmability (**Figure 28**).



**Figure 28** Diverse patterned deformation of the pixelated mechanical metamaterial.

### 3.3. Fixation of the compressed domain of metamaterial

#### 3.3.1. Reconfiguration cycle

The metamaterial under the room temperature is in the initial state, and the voids are rigid as the stiffness of the embedded phase-transition layer. The selected domain was activated and waited for the phase transition of the LMPA layer for several minutes. After the LMPA layer melts into a liquid, the activated domain can be deformed due to the compliant stiffness of the layer. Furthermore, this deformed state can be fixed by removing the applied voltage while maintaining compression (**Figure 29**). This is because solidified LMPA layers are rigid enough to maintain the deformation and to exceed the elastic force of the soft silicone layer that returns to its original shape. The recovery of the shape of the metamaterial to its initial state by activating the deformed domain is also possible through electrical stimulus.

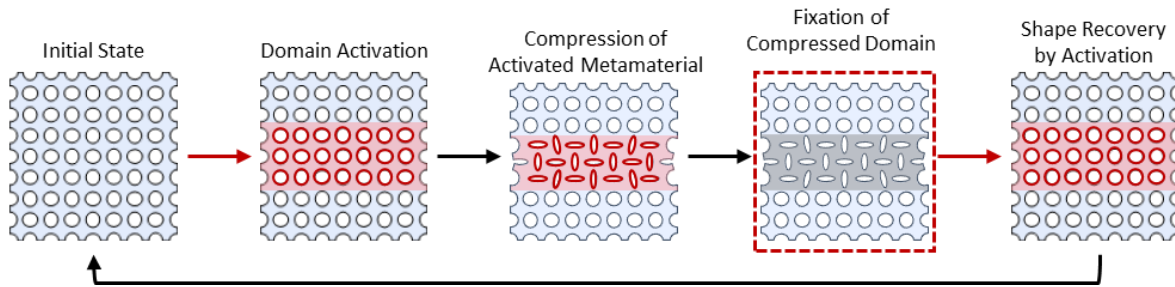


**Figure 29** Compressed domain can be fixed through cooling the activated domain while maintaining the applied pressure.

#### 3.3.2. Fixation of domain deformation of metamaterial

Four of the patterned deformation has fixed; 1) buckling of the whole domain, 2) buckling of four rows, 3) buckling of three rows in the middle, and 4) buckling of the voids at three by three corner. When the whole voids in the metamaterial are deformed and fixed, the material would have a single domain without any boundary. For fixation of the patterned domain, the structure presents two or three domains (**Figure 30**).

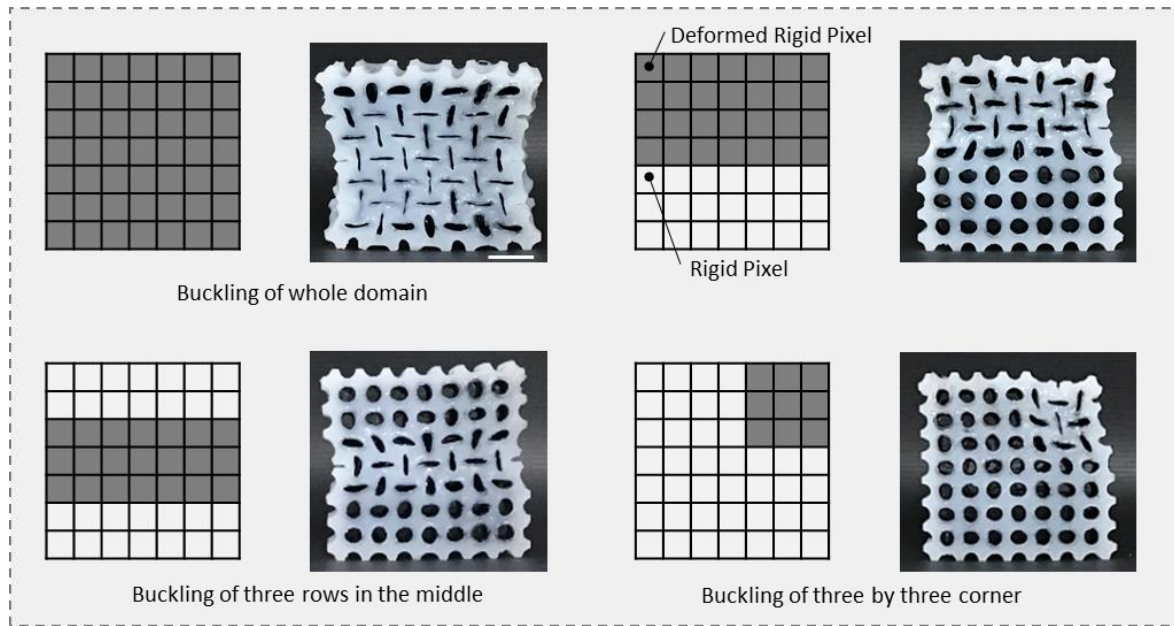


**Figure 30** Four different patterned deformations are fixed.

### 3.4. Conclusion

The pixelated mechanical metamaterial is locally addressable and programmable soft material-based system, which exhibits negative Poisson's ratio behavior for the activated domain. The metamaterial successfully conducts patterned deformation and fixation of patterned deformation. Also, the electrical and thermal properties of structure and layers were analyzed. The system well-established the coupling of auxetic structure and material characteristics. In sum, the metamaterial can change the rigidity of the selected domain through local activation and can fix the patterned deformation. In a further study, our system could be applied to the stiffness tuning the soft-material system with higher programmability of its mechanical characteristics.

## CHAPTER 4 Poisson's ratio & analysis

### 4.1. Calculation of Poisson's ratio

The Poisson's ratio was measured along with the strain of the deformed structure through the manual calculation with the captured images of the deformation video. Sixteen vertices around the nine central voids were tracked to get local values of strain in both x and y directions.  $X_{i0}$  and  $Y_{i0}$  were measured, which are the length between the two vertices before deformation, and the  $X_i$  and  $Y_i$  were also measured, which are the length after the deformation of the metamaterial, where  $i=1,2,3$ , and 4. The local Poisson's ratios have calculated from,

$$v_i = - (X_{i0} - X_i) / (Y_{i0} - Y_i).$$

The final value of the Poisson's ratio was calculated from the average of the local Poisson's ratio values (Figure 31).

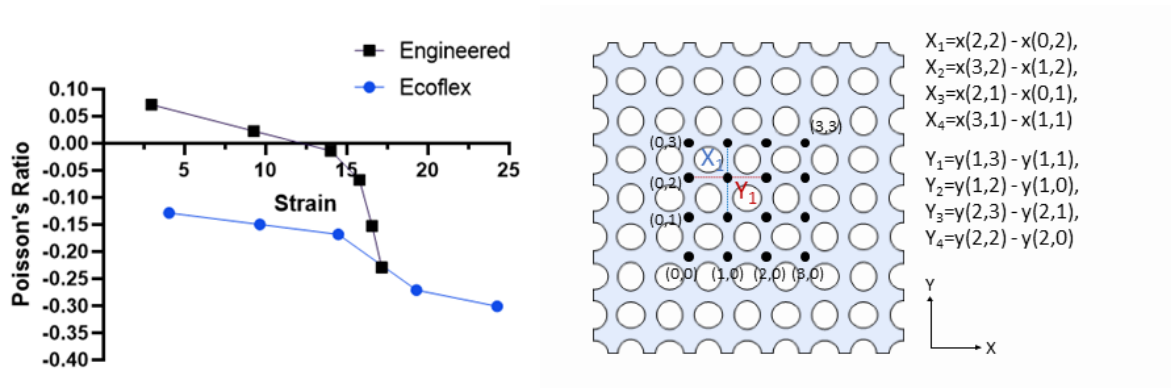


**Figure 31** The engineered metamaterial and the silicone rubber metamaterial's Poisson's ratio were measured along with the strain of the structure. The silicone rubber structure shows more negative Poisson's ratio behavior than the engineered counterpart.

### 4.2. Comparison between silicone rubber metamaterial and engineered metamaterial

The metamaterial that is made of only silicone rubber (Ecoflex 00-30, Smooth-On) was prepared to compare the deformation under the uniaxial compression with the engineered metamaterial. The distinctive difference between the two structures is the stiffness of the structure due to the absence of a phase-transition layer in silicone rubber metamaterial. We have calculated Poisson's ration from 16 vertices around the nine representative voids of two structures with strain changes. The Poisson's ratio of the engineered metamaterial in which every void of the structure is activated was positive until the strain reaches about 13%. However, the Poisson's ratio drastically dropped after it turned to a negative value and caught up with the value of silicone rubber structure's Poisson's ratio. Unlike pixelated

metamaterial, Poisson's ratio of the silicone rubber metamaterial gradually decreases as the strain of the structure increases from 4% to 24% (**figure 32**).

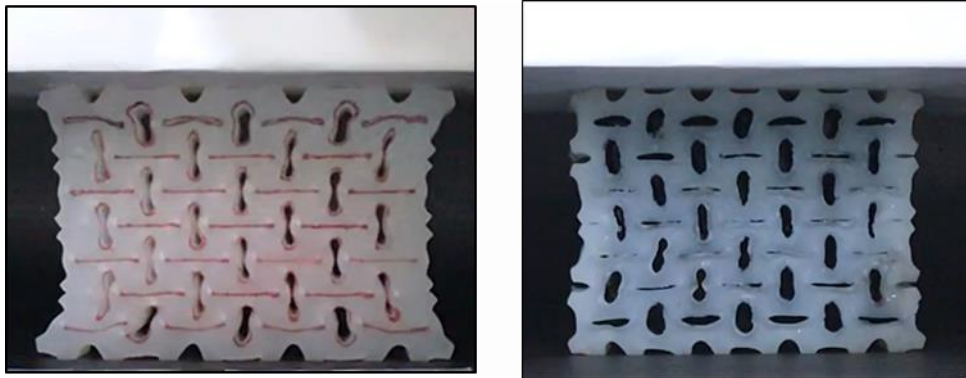


**Figure 32** Silicone rubber metamaterial shows more negative Poisson's ratio behavior than the engineered metamaterial.

When all of the voids in the engineered metamaterial are activated, the structure can exhibit elastic instability under uniaxial pressure. Similarly, silicone rubber metamaterial displays buckling behavior under compression. Yet, the difference between the two metamaterials arises from the dissimilar material characteristics such as bulk modulus of silicone rubber and LMPA. The different materialistic properties led to dissimilar elastic instability in two structures. The silicone rubber metamaterial shows clear negative Poisson's ratio behavior under uniaxial compression, whereas the engineered metamaterial is not able to show clear negative Poisson's ratio behavior since the effect of the embedded liquid LMPA layers.

## **CHAPTER 5 Concluding remarks**

This chapter will describe the summary of the research, advantages, and limitation of the work, and future prospects.

### **5.1 Summary of the work**

I developed mechanical metamaterials with periodic void units embedding the LMPA layer to change local stiffness. Through electrical activation, I could change the stiffness of pixels, and deform and restore the structure. Furthermore, I could demonstrate various patterned deformations by choosing which pixels to activate, as well as fixing the deformed shape of the structure. This shape fixation was possible by deactivating and cooling the activated pixels during deformation. When the deformation of engineered mechanical metamaterial and soft silicone rubber metamaterial were compared, there was a difference in Poisson's ratio due to the pressure of liquid LMPA layer in engineered structure.

### **5.2 Future prospect**

For future work, the desirable mechanical metamaterial is to scale down the structure for saving manufacturing costs, making a size effect (e.g. higher strength when the structure is in nanoscale.), and higher resolution of programming. We could think of using other material compositions, structures, and stimuli for pixelated activation interface for diverse applications.



## References

1. Yu, X., Zhou, J., Liang, H., Jiang, Z., & Wu, L. (2018). Mechanical metamaterials associated with stiffness, rigidity and compressibility: A brief review. *Progress in Materials Science*, 94, 114-173.
2. Surjadi, J. U., Gao, L., Du, H., Li, X., Xiong, X., Fang, N. X., & Lu, Y. (2019). Mechanical metamaterials and their engineering applications. *Advanced Engineering Materials*, 21(3), 1800864.
3. Bell, A. G. (1903). *The tetrahedral principle in kite structure*. Judd & Detweiler.
4. Zadpoor, A. A. (2016). Mechanical meta-materials. *Materials Horizons*, 3(5), 371-381.
5. G. W. Milton and A. V. Cherkaev, Which elasticity tensors are realizable?, *J. Eng. Mater. Technol.*, 1995, 117, 483–493
6. Kadic, M., Bückmann, T., Stenger, N., Thiel, M., & Wegener, M. (2012). On the practicability of pentamode mechanical metamaterials. *Applied Physics Letters*, 100(19), 191901.
7. Bückmann, T., Schittny, R., Thiel, M., Kadic, M., Milton, G. W., & Wegener, M. (2014). On three-dimensional dilational elastic metamaterials. *New Journal of Physics*, 16(3), 033032.
8. Wang, Y. C., & Lakes, R. S. (2005). Composites with inclusions of negative bulk modulus: extreme damping and negative Poisson's ratio. *Journal of Composite Materials*, 39(18), 1645-1657.
9. Klatt, T., & Haberman, M. R. (2013). A nonlinear negative stiffness metamaterial unit cell and small-on-large multiscale material model. *Journal of Applied Physics*, 114(3), 033503.
10. Wang, Y. C., & Lakes, R. S. (2004). Extreme stiffness systems due to negative stiffness elements. *American Journal of Physics*, 72(1), 40-50.
11. Correa, D. M., Seepersad, C. C., & Haberman, M. R. (2015). Mechanical design of negative stiffness honeycomb materials. *Integrating Materials and Manufacturing Innovation*, 4(1), 10.
12. Felton, S., Tolley, M., Demaine, E., Rus, D., & Wood, R. (2014). A method for building self-folding machines. *Science*, 345(6197), 644-646.
13. Kuribayashi, K., Tsuchiya, K., & You, Z. (2006). Dacian Tomus, Minoru Umemoto, Takahiro Ito, and Masahiro Sasaki. Self-deployable origami stent grafts as a biomedical application of ni-rich tni shape memory alloy foil. *Materials Science and Engineering: A*, 419(1-2), 131-137.

14. Lv, C., Krishnaraju, D., Konjevod, G., Yu, H., & Jiang, H. (2014). Origami based mechanical metamaterials. *Scientific reports*, 4, 5979.
15. Schenk, M., & Guest, S. D. (2013). Geometry of Miura-folded metamaterials. *Proceedings of the National Academy of Sciences*, 110(9), 3276-3281.
16. Silverberg, J. L., Evans, A. A., McLeod, L., Hayward, R. C., Hull, T., Santangelo, C. D., & Cohen, I. (2014). Using origami design principles to fold reprogrammable mechanical metamaterials. *science*, 345(6197), 647-650.
17. Jackson, J. A., Messner, M. C., Dudukovic, N. A., Smith, W. L., Bekker, L., Moran, B., ... & Spadaccini, C. M. (2018). Field responsive mechanical metamaterials. *Science advances*, 4(12), eaau6419.
18. Yang, D., Jin, L., Martinez, R. V., Bertoldi, K., Whitesides, G. M., & Suo, Z. (2016). Phase-transforming and switchable metamaterials. *Extreme Mechanics Letters*, 6, 1-9.
19. Yang, C., Boorugu, M., Dopp, A., Ren, J., Martin, R., Han, D., ... & Lee, H. (2019). 4D printing reconfigurable, deployable and mechanically tunable metamaterials. *Materials Horizons*.
20. Gladman, A. S., Matsumoto, E. A., Nuzzo, R. G., Mahadevan, L., & Lewis, J. A. (2016). Biomimetic 4D printing. *Nature materials*, 15(4), 413.
21. Alderson, A., Rasburn, J., Ameer-Beg, S., Mullarkey, P. G., Perrie, W., & Evans, K. E. (2000). An auxetic filter: a tuneable filter displaying enhanced size selectivity or defouling properties. *Industrial & engineering chemistry research*, 39(3), 654-665.
22. Yufei, H., Tianmiao, W., Xi, F., Kang, Y., Ling, M., Juan, G., & Li, W. (2017, July). A variable stiffness soft robotic gripper with low-melting-point alloy. In *2017 36th Chinese Control Conference (CCC)* (pp. 6781-6786). IEEE.
23. Shintake, J., Schubert, B., Rosset, S., Shea, H., & Floreano, D. (2015, September). Variable stiffness actuator for soft robotics using dielectric elastomer and low-melting-point alloy. In *2015 IEEE/RSJ International Conference on Intelligent Robots and Systems (IROS)* (pp. 1097-1102). IEEE.
24. Bertoldi, K., Reis, P. M., Willshaw, S., & Mullin, T. (2010). Negative Poisson's ratio behavior induced by an elastic instability. *Advanced materials*, 22(3), 361-366.
25. Overvelde, J. T., Shan, S., & Bertoldi, K. (2012). Compaction through buckling in 2D periodic, soft and porous structures: effect of pore shape. *Advanced Materials*, 24(17), 2337-2342.
26. Shim, J., Shan, S., Košmrlj, A., Kang, S. H., Chen, E. R., Weaver, J. C., & Bertoldi, K. (2013).

Harnessing instabilities for design of soft reconfigurable auxetic/chiral materials. *Soft Matter*, 9(34), 8198-8202.

## Acknowledgment

I would like to express my special gratitude to my undergraduate intern and master's advisor, **professor Jiyeon Kim**, who has been always guided me with insight and teach me attitude that is not only for research, but also handling challenges. She helped me more than anyone, always amend my weakness in academic researches. She showed the way how to progress the work, and gave me encouragement and advices, which have been an invaluable support for me during my study. Without her guidance, it must be impossible to complete the dissertation, as well as to develop an idea of this project.

I am grateful to all of those with whom helped me to finish the work and do not hesitate to give helpful advices on my work. I would like to thanks to **professor Moon Kee Choi** and **professor Young Chul Jun**, who gave me new insights and perspective during thesis defense. I am grateful for their advices, encouragement, and guidance to make development for my work.

Also, I want to appreciate to our laboratory members who helped me with conducting experiments. Thanks to **Jun Kyu Choe**, who developed simulation of pixelated mechanical metamaterials, and **Yeonwoo Chang**, who aid me in take videos of the structure during deformation experiments. With their help, I could finish this thesis.

Finally, I feel thankful to **my family** who gives me an unlimited support while I do my study.

With sincere regards,

**Jeeyoon Yi**

## Curriculum Vitae

Jeeyoon Yi

Ulsan National Institute of Science and Technology

50, UNIST-gil, Ulsan 44919, Republic of Korea

Tel: +82-10-4383-2283 / [dbsl52792@gmail.com](mailto:dbsl52792@gmail.com)

### EDUCATION

---

**Ulsan National Institute of Science and Technology (UNIST), Ulsan, Korea (Feb. 2018 – Present)**

**M.S. in Materials Science and Engineering**

- Studied engineered mechanical metamaterials with programmable local stiffness of pixelated units. Each pixel can be activated through electrical stimulus and deformed under uniaxial compression when activated.
- **Thesis:** “*Programmable activation of mechanical metamaterial using stiffness controllable mechanical pixels. (expected)*”
- Advisor: Jiyun Kim

**Ulsan National Institute of Science and Technology (UNIST), Ulsan, Korea (Mar. 2013 – Feb. 2018)**

**B.S. in Nano Materials Engineering / Advanced Materials Science**

- Superior Award for superior semester grades for 2 out of 8 semesters

### SCHOLARSHIPS

---

- Awarded full-tuition scholarships for 4 out of 4 semesters

**Feb. 2018 – Present**

- Awarded full-tuition scholarships for 7 out of 8 semesters

**Mar. 2013 – Dec. 2017**

### RESEARCH EXPERIENCE

---

**Materials Intelligence Laboratory, Ulsan, Korea (Advisor: Jiyun Kim) (Feb. 2017 – Present)**  
**M.S. & B.S.**

- Developed the system that coupled the auxetic material and the characteristics of materials with locally programmable stiffness of mechanical metamaterials.
- Conducted experiments to develop magnetically and thermally controllable tensegrity.
- Fabricated diverse scaled thermal and magnetic responsive actuators through mixing up magnetic particles, thermal responsive particles, and soft silicone rubber.
- Applied and practiced 3D designing and 3D printing for mold fabrications.
- Joined in the project of manipulation of the collective soft magnetic actuator group on the surface of the water and analyzed the data.
- Practiced mammalian cell culturing and passaging in several different environments.

## **PRESENTATIONS**

---

- **Jeeyoon Yi**, Suwoo Lee, Hajun Lee, and Jiyun Kim\*, “Electrically assignable auxetic materials with programmable mechanical properties”(Oral Presentation), Nano Korea 2019, **Jul. 2019**

## **PATENT APPLICATIONS**

---

- Shape variable composite and manufacturing method for the same. Kim, J. Y.; **Yi, J. Y.**; Choe, J.K.; Jang, Y. W.; Song, H. S. Korean Patent 10-2019-0156157(2019).
- Soft magnetic composite and preparation method thereof. Kim, J. Y.; Kwon, M. S.; Yoo J. W.;...; **Yi, J. Y.**; Park, S. H. Korean Patent 10-2019-0150651(2019).

## **SKILLS**

---

- Rigorously following lab protocol and experimental procedure
- 3D Printing (Ultimaker2 / Formlab)
- 3D Designing and modeling (3ds Max 2018)
- Culturing and passaging the mammalian cells
- Language: Korean (Native), English (Advanced), Chinese (Beginner)

